Supporting Information

Synthesis and characterization of disiloxane cross-linked polysulfides

Kun Woo Park, Zoran Zujovic and Erin M. Leitao*

School of Chemical Sciences, University of Auckland, Private Bag, 92019, Auckland, 1142, New Zealand

Spectra:

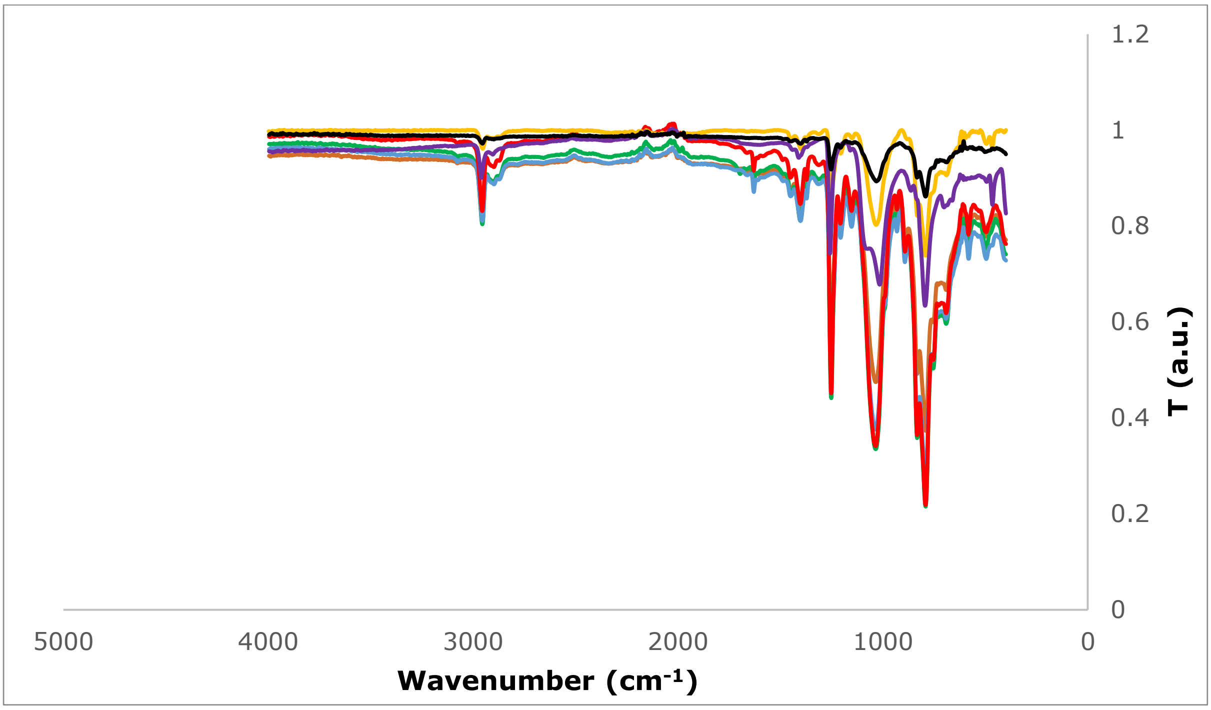

Figure S1: FTIR spectra of X-poly-(S-*r*-allyldisiloxane), X = 33 wt% S (black), X = 37 wt% S (red), X = 40 wt% S (blue), X = 45 wt% S (green), X = 50 wt% S (orange), X = 70 wt% S (gold) and X = 90 wt% S (purple).

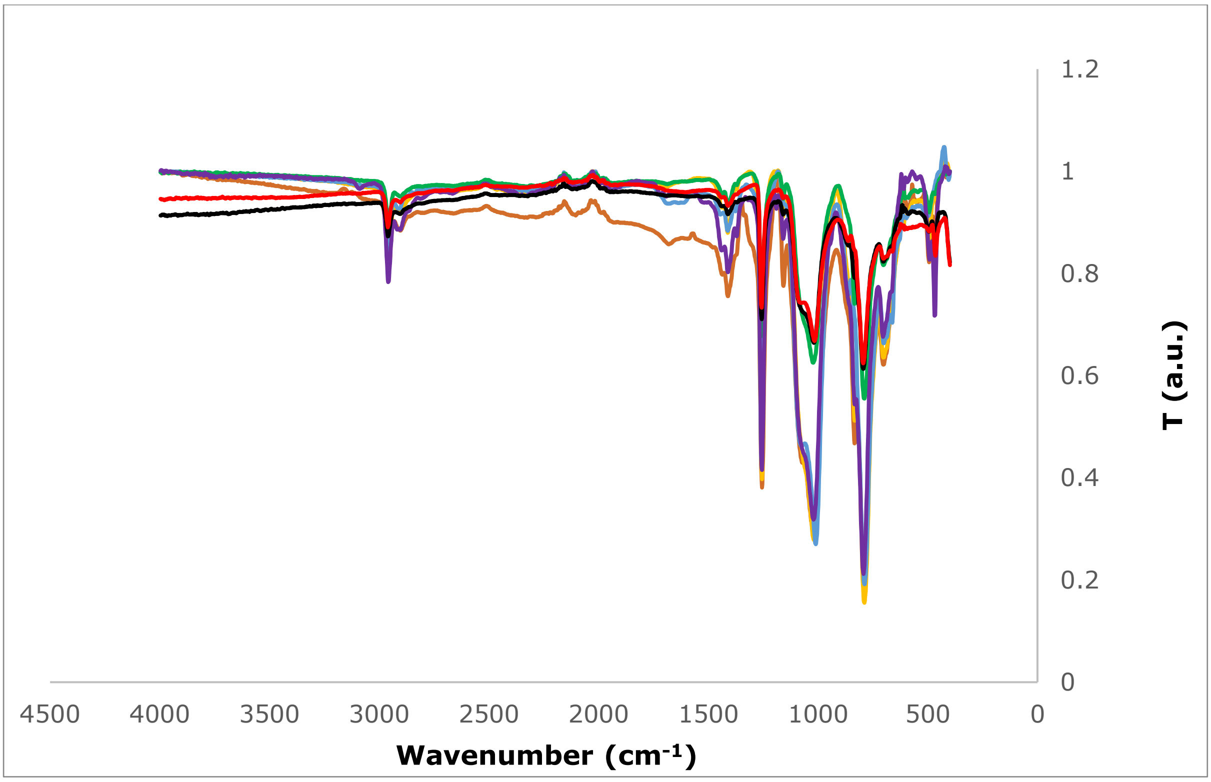

Figure S2: FTIR spectra of X-poly-(S-*r*-vinyldisiloxane), X = 30 wt% S (blue), X = 40 wt% S (yellow), X = 50 wt% S (brown), X = 60 wt% S (green), X = 70 wt% S (purple), X = 80 wt% S (black) and X = 90 wt% S (red).

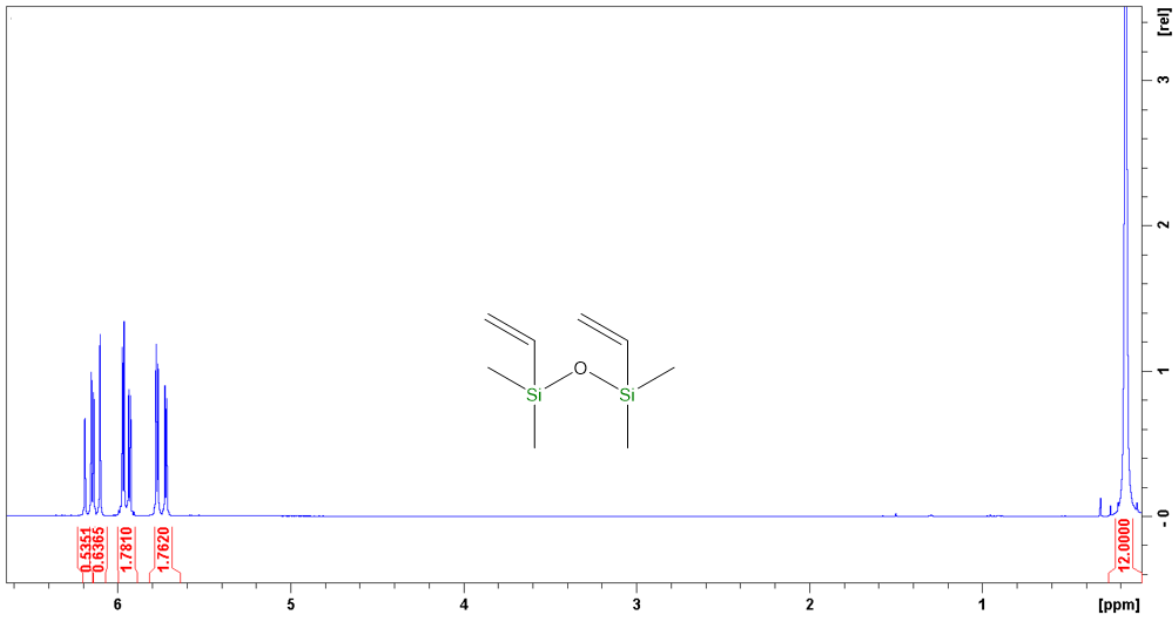

Figure S3: ^{1}H NMR spectrum of 1,3-divinyl-tetramethyldisiloxane, in $CDCl_3$.

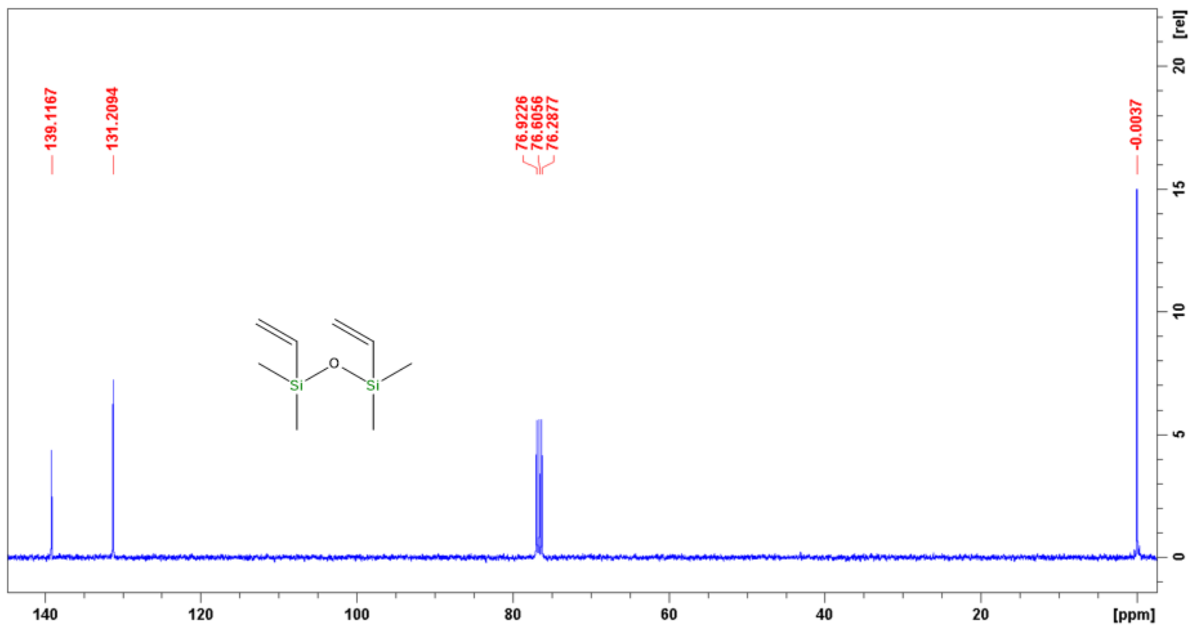

Figure S4: $^{13}C\{^{1}H\}$ NMR spectrum of 1,3-divinyl-tetramethyldisiloxane, in $CDCl_3$.

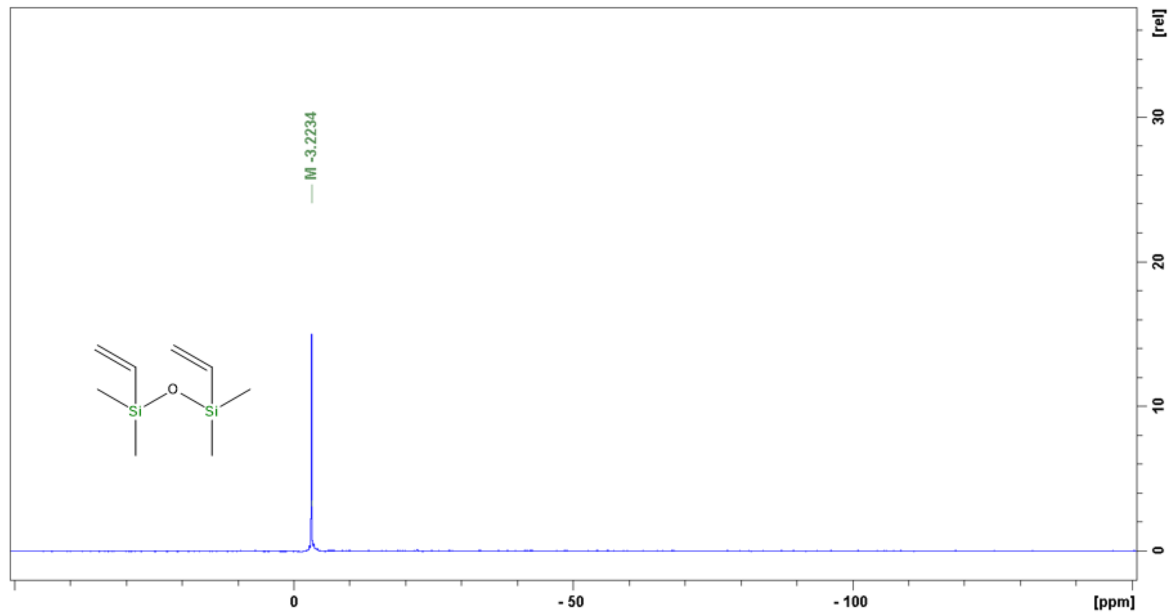

Figure S5: $^{29}Si\{^{1}H\}$ NMR spectrum of 1,3-divinyl-tetramethyldisiloxane, in $CDCl_3$.

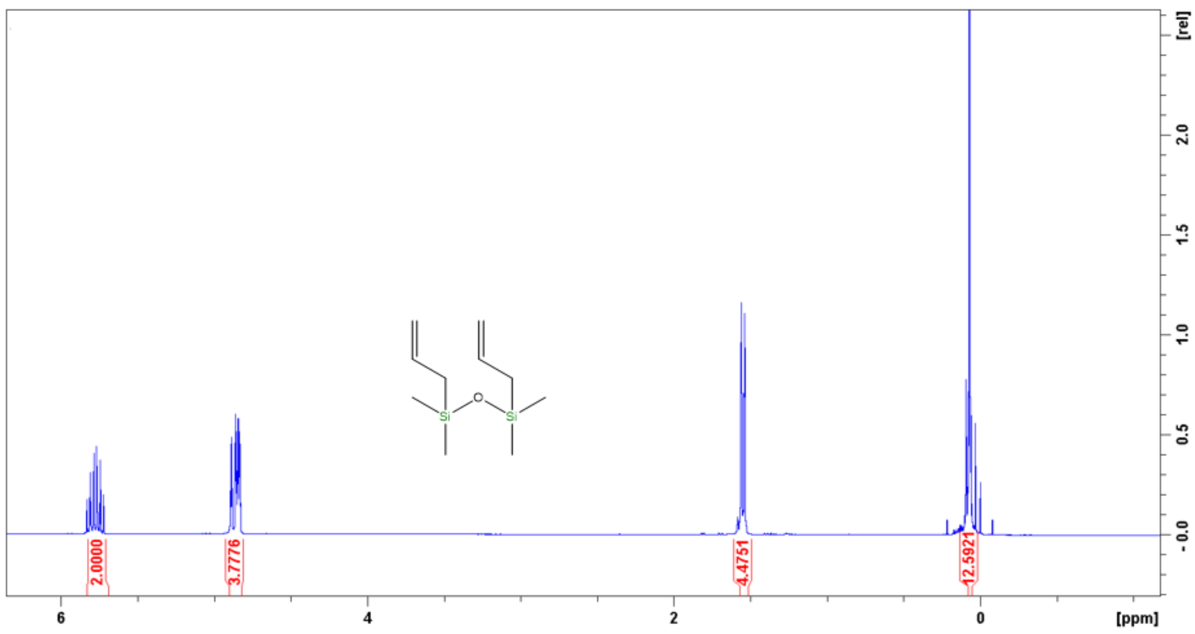

Figure S6: ^{1}H NMR spectrum of 1,3-diallyl-tetramethyldisiloxane, in $CDCl_3$.

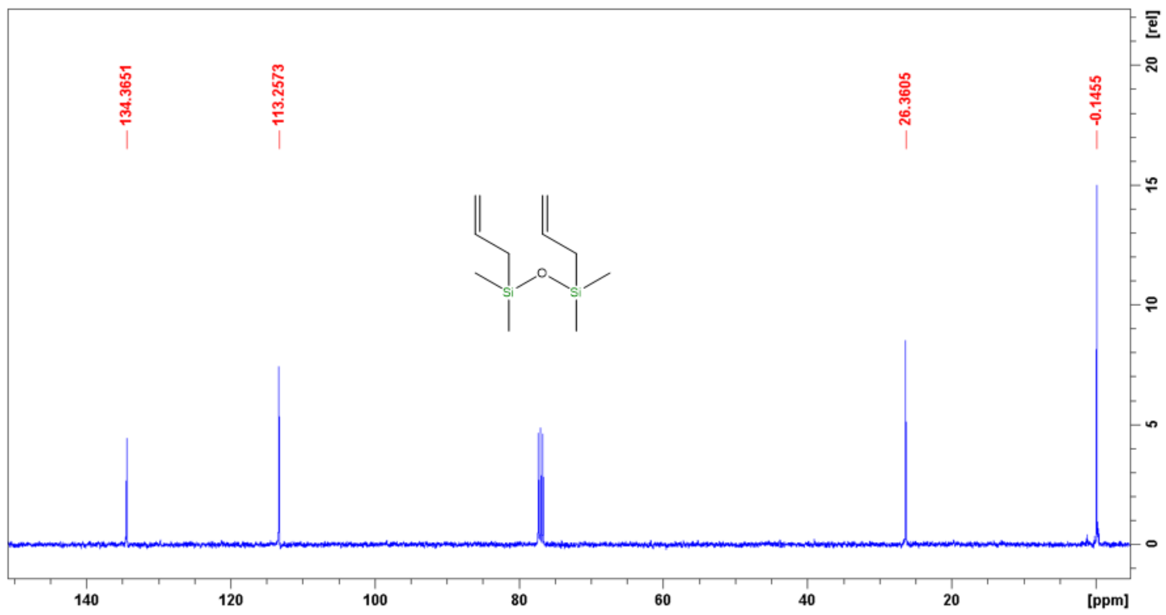

Figure S7: $^{13}C\{^{1}H\}$ NMR spectrum of 1,3-diallyl-tetramethyldisiloxane, in $CDCl_3$.

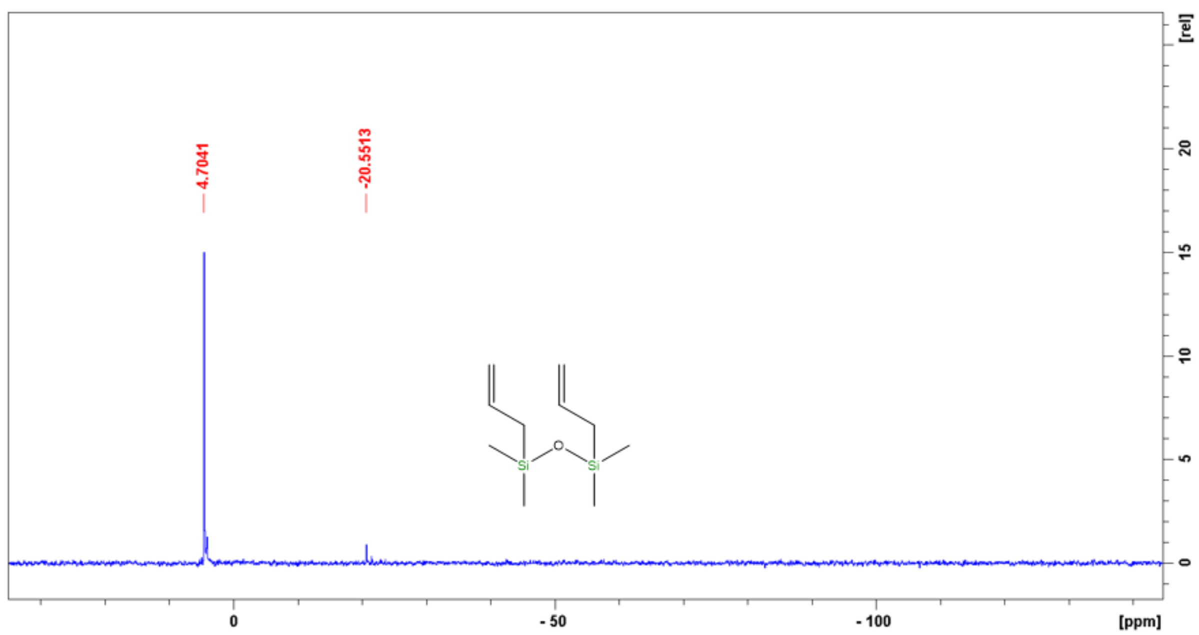

Figure S8: $^{29}Si\{^{1}H\}$ NMR spectrum of 1,3-divinyl-tetramethyldisiloxane, in $CDCl_3$. Peak at -20.5 ppm corresponds to silicon grease.

Figure S9: Photo of X-poly(S-r-allyldisiloxane) series (X = wt% S). From left to right: X = 33, 37, 40, 45, 50, 70 and 90.

Figure S10: Photo of X-poly(S-r-vinyldisiloxane) series (X = wt% S). From left to right: X = 30, 40, 50, 60, 70, 80, 90.

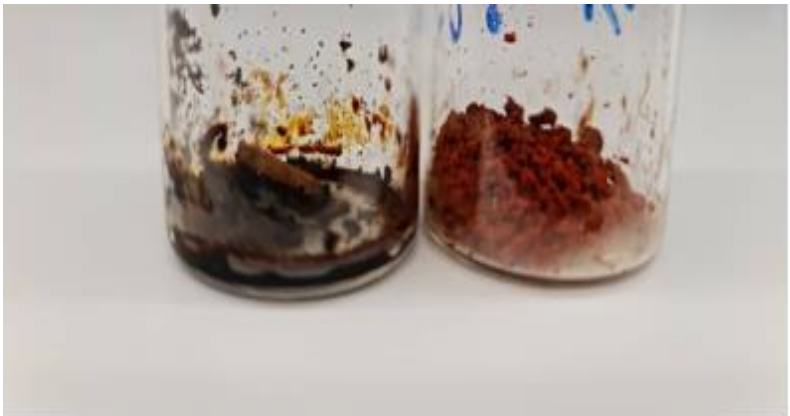

Figure S11: 37-poly-(S-r-allyldisiloxane) synthesized using Grignard route (left) and hydrolysis pathway (right).

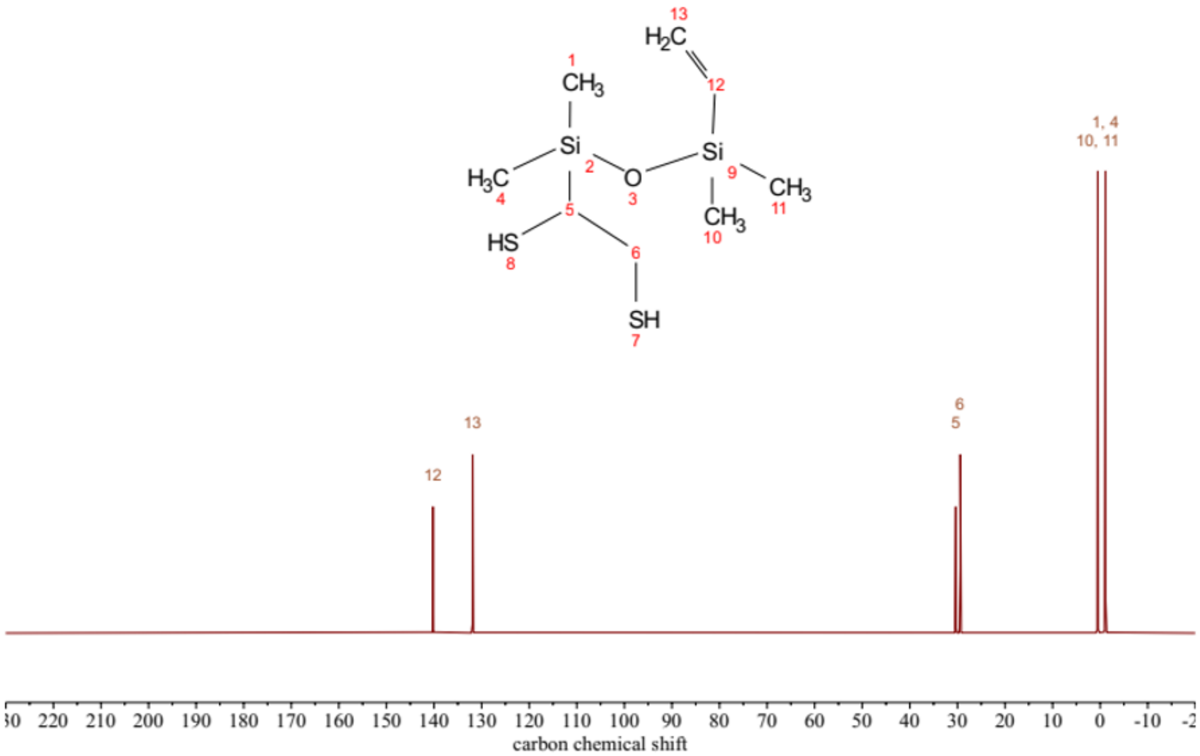

Figure S12: Predicted ^{13}C NMR spectrum of the X-poly(S-*r*-vinyldisiloxane) series

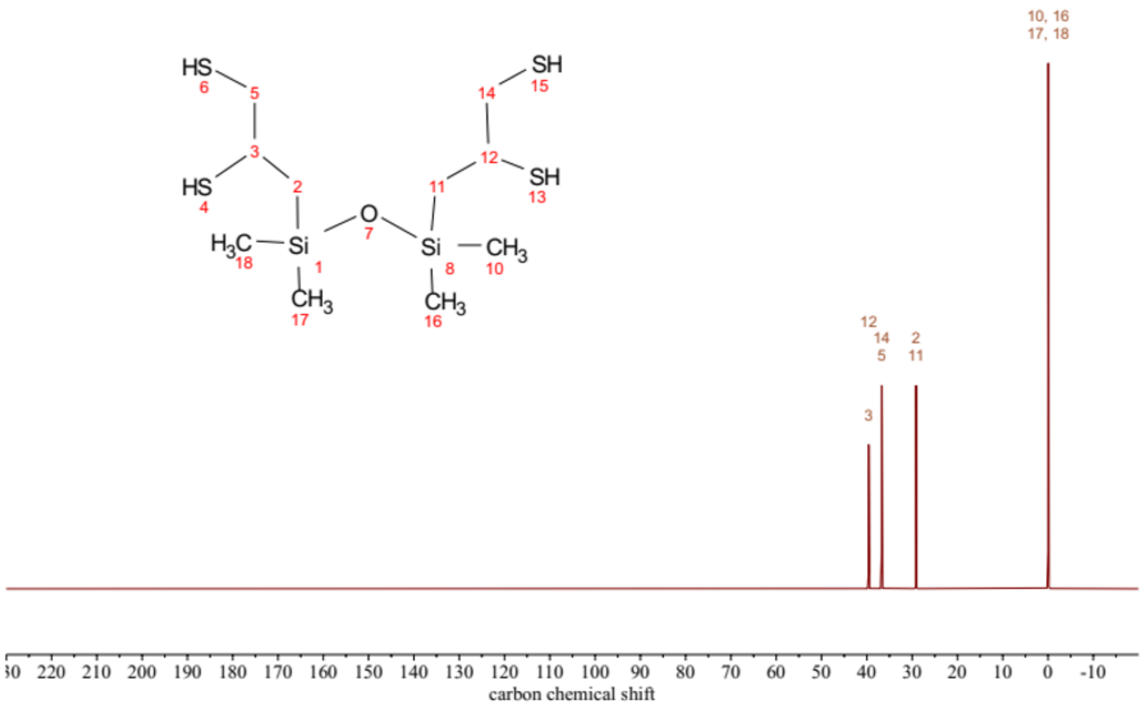

Figure S13: Predicted ^{13}C NMR spectrum of the X-poly(S-*r*-allyldisiloxane) series

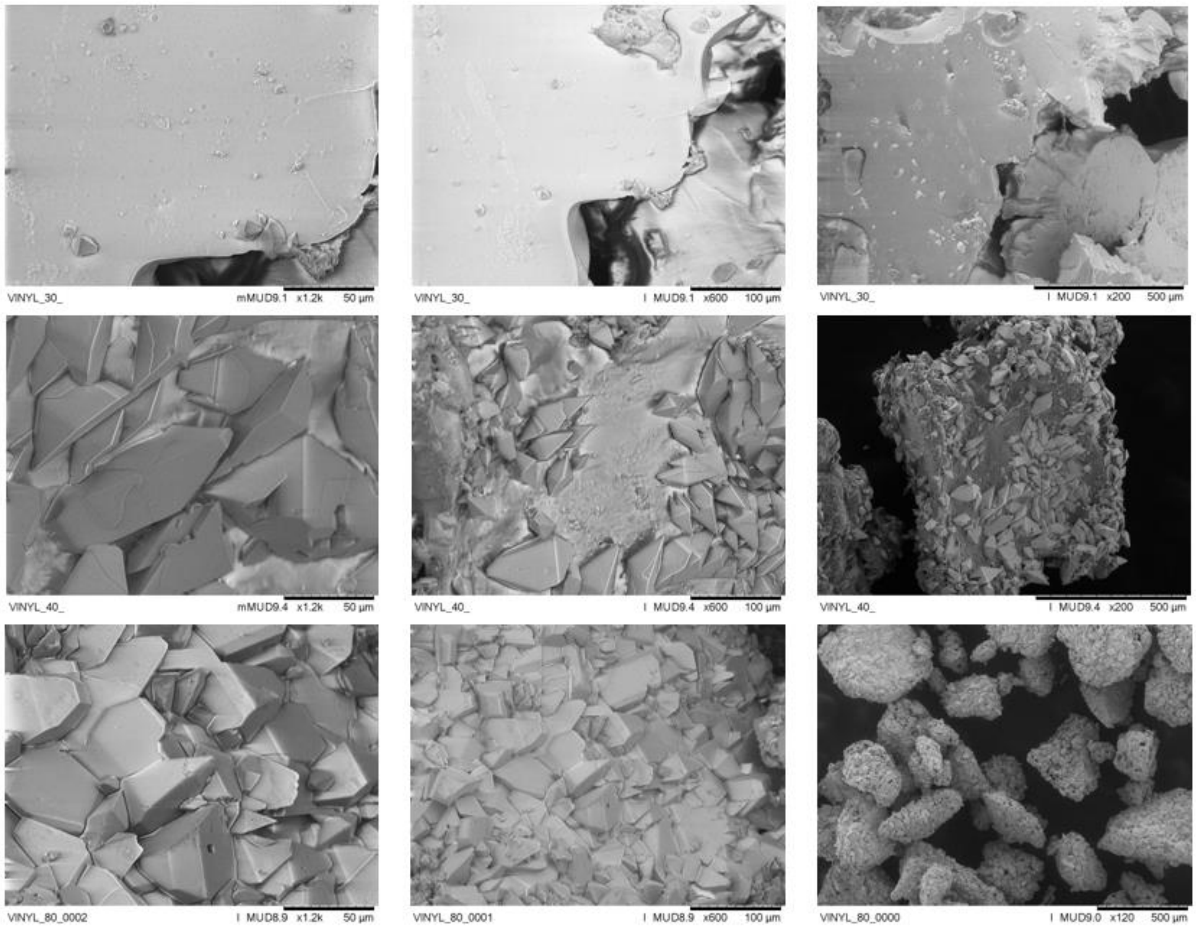

Figure S14: Representative SEM images for different wt% S polysulfides; top row: 30-poly(S-*r*-vinyldisiloxane), middle row: 40-poly(S-*r*-vinyldisiloxane), bottom row: 80-poly(S-*r*-vinyldisiloxane).

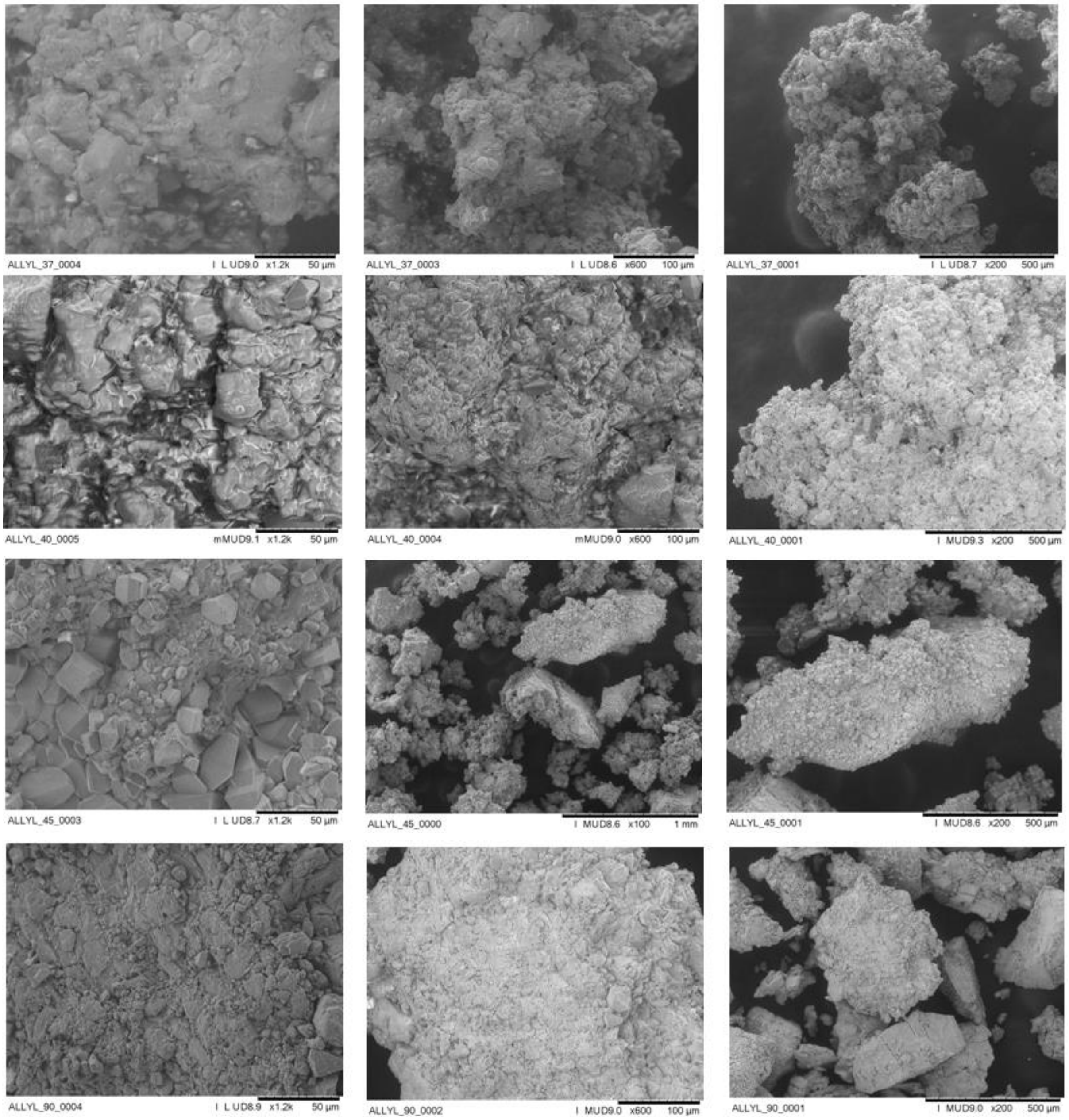

Figure S15: Representative SEM images for different wt% S polysulfides; down the image from top row, 37-poly(S-*r*-allyldisiloxane), 40-poly(S-*r*-allyldisiloxane) and 45-poly(S-*r*-allyldisiloxane), 90-poly(S-*r*-allyldisiloxane).

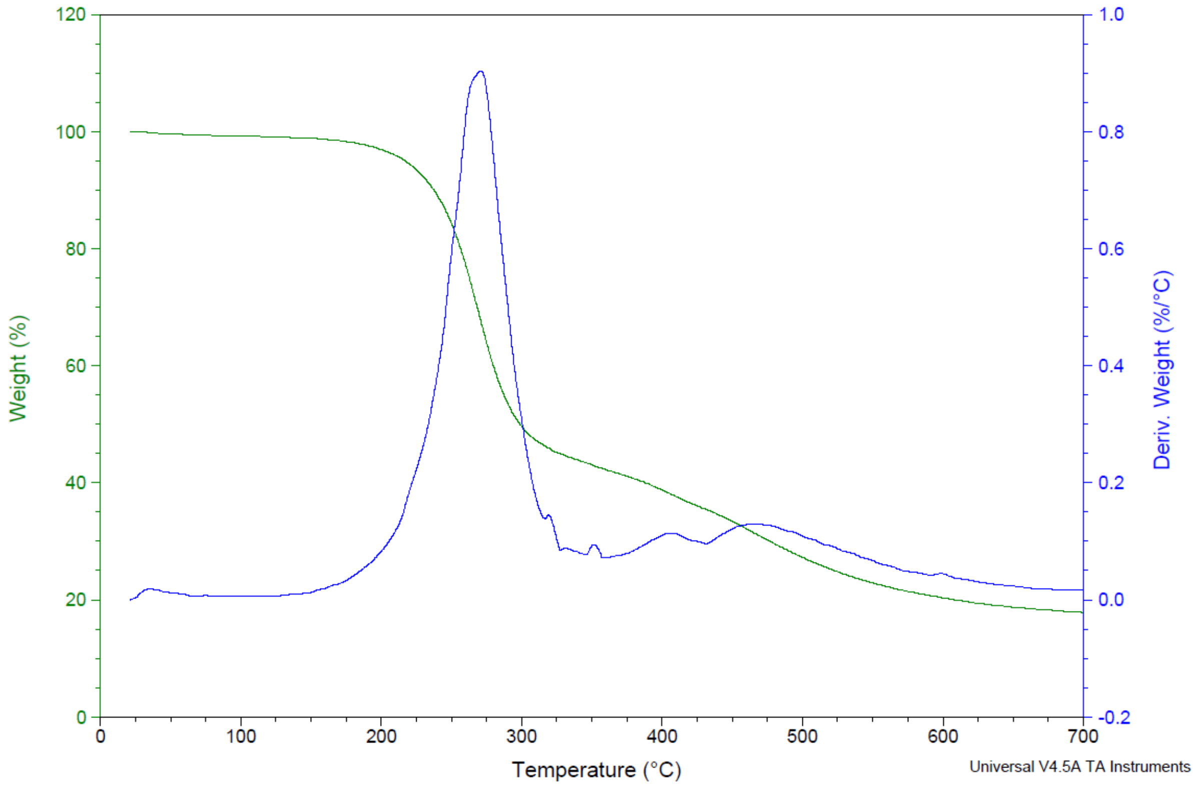

Figure S16: TGA scan of 30-poly(S-*r*-vinyldisiloxane). Degradation begins to occur at 200°C. This is indicative of the sulfur domains beginning to degrade.

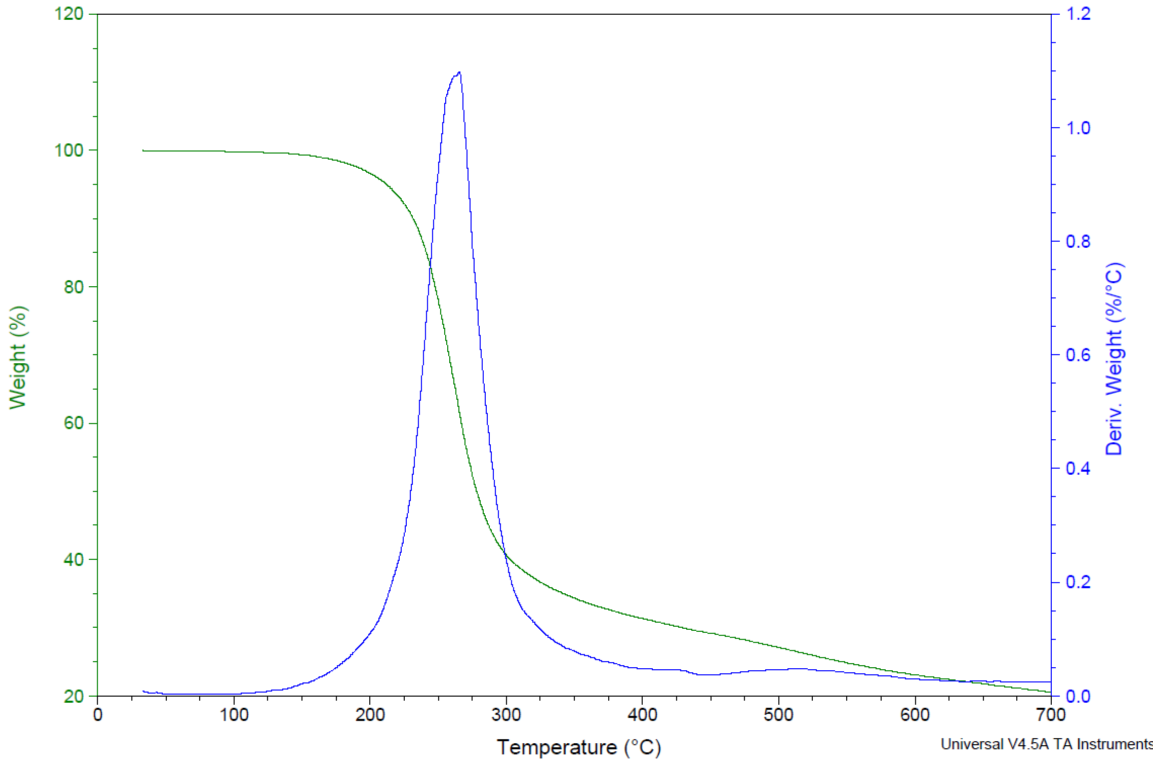

Figure S17: TGA scan of 40-poly(S-*r*-vinyldisiloxane). Degradation begins to occur at 200°C. This is indicative of the sulfur domains beginning to degrade.

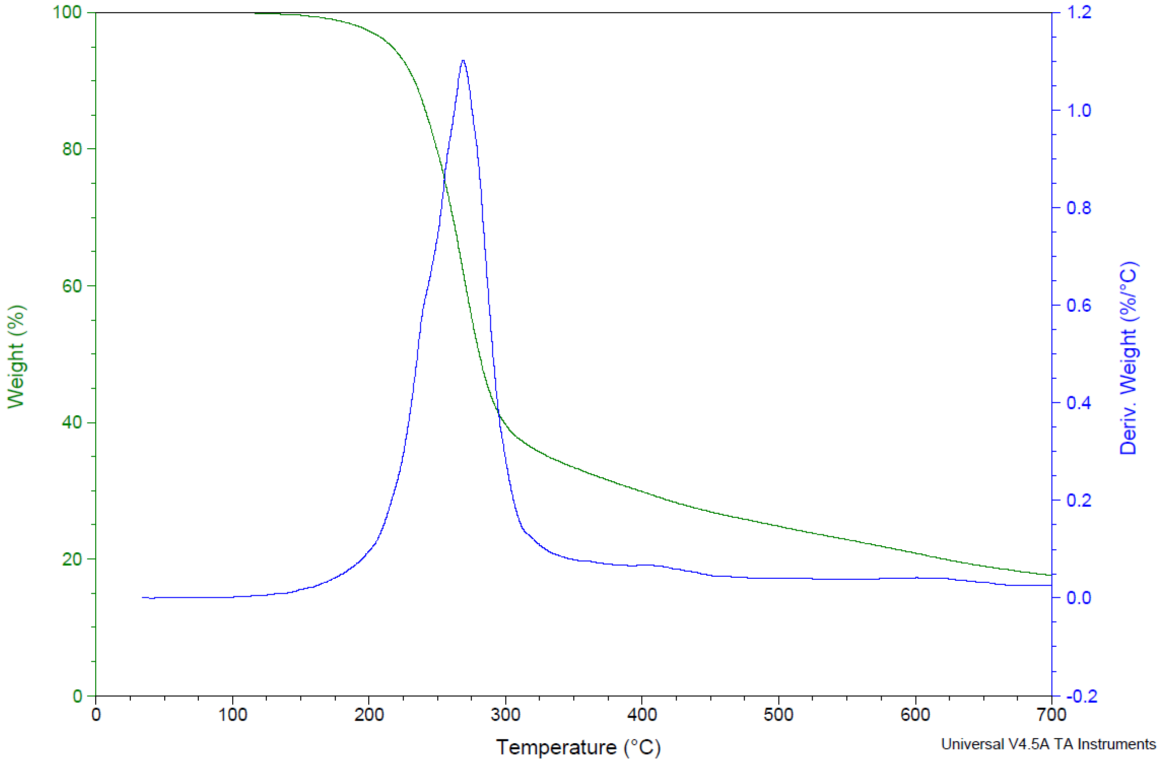

Figure S18: TGA scan of 50-poly(S-*r*-vinyldisiloxane). Degradation begins to occur at 200°C. This is indicative of the sulfur domains beginning to degrade.

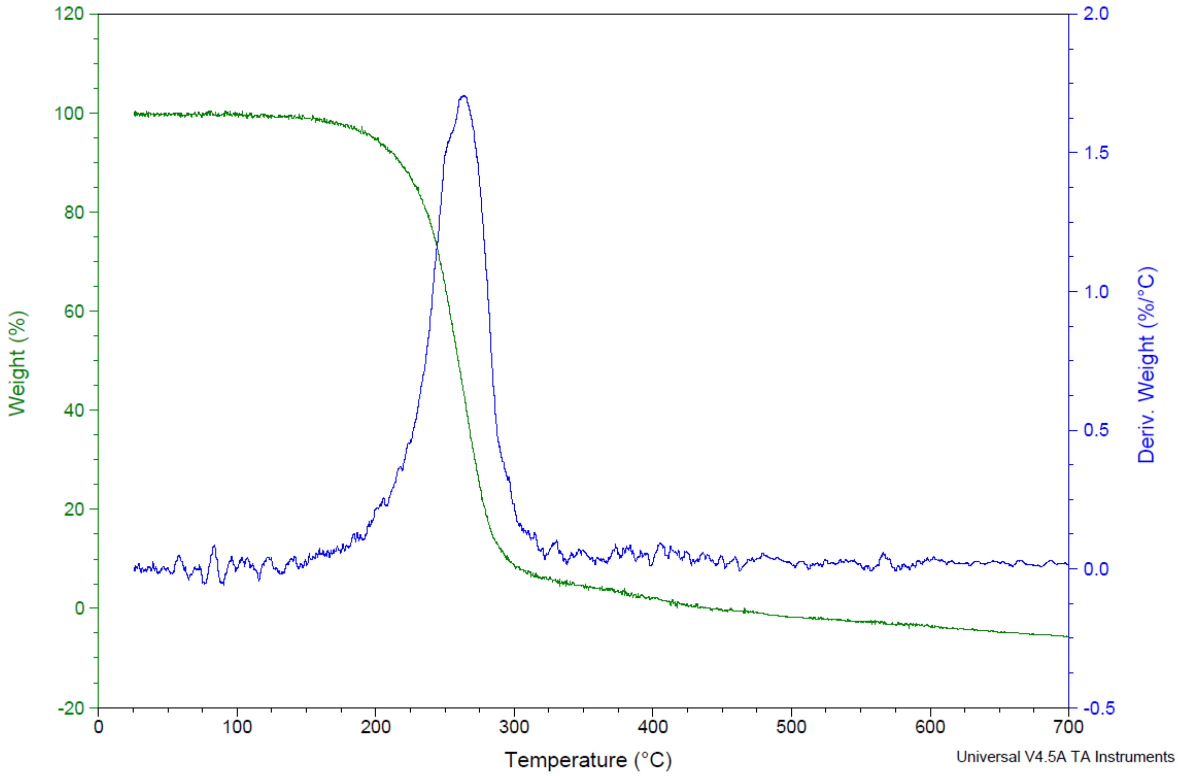

Figure S19: TGA scan of 60-poly(S-*r*-vinyldisiloxane). Degradation begins to occur at 200°C. This is indicative of the sulfur domains beginning to degrade.

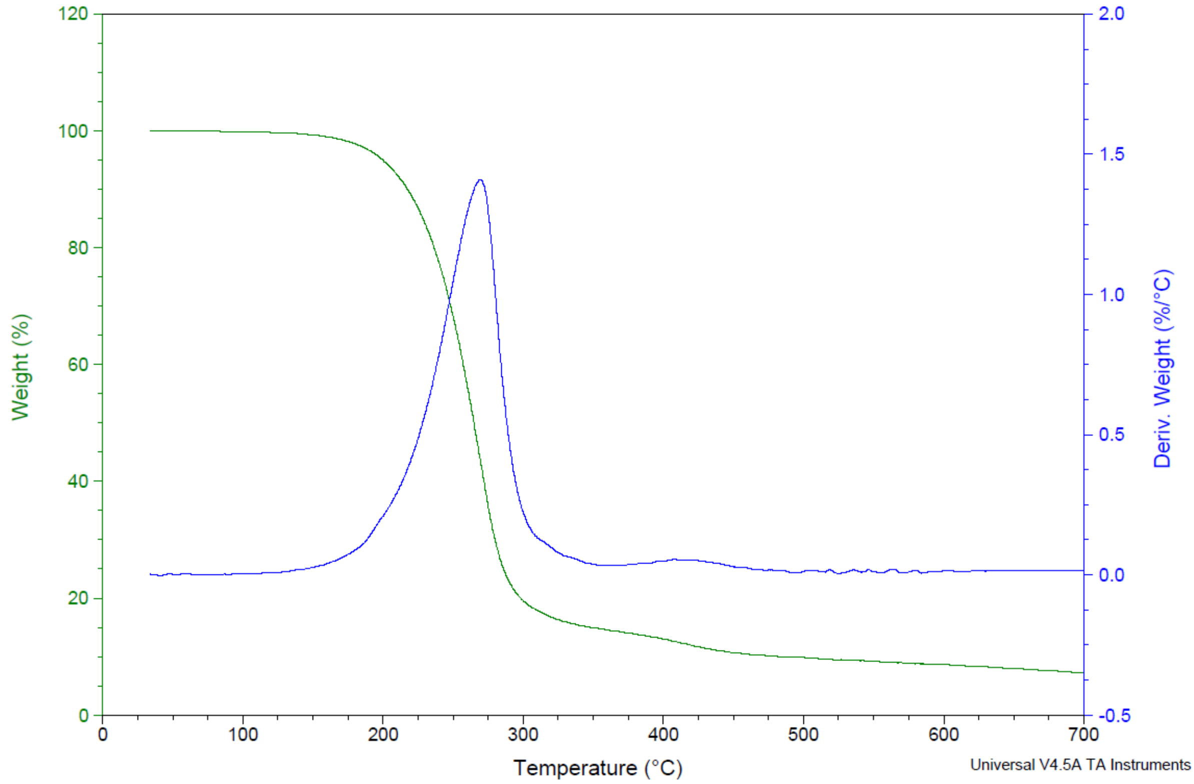

Figure S20: TGA scan of 70-poly(S-*r*-vinyldisiloxane). Degradation begins to occur at 200°C. This is indicative of the sulfur domains beginning to degrade.

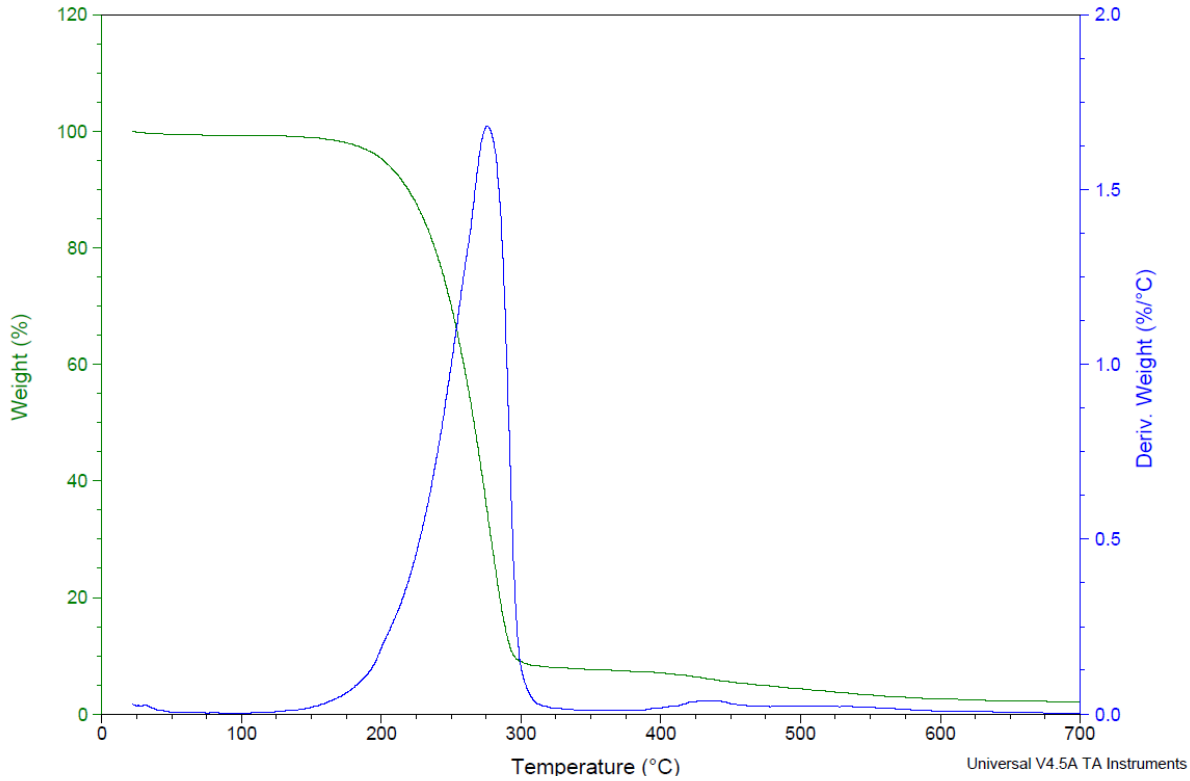

Figure S21: TGA scan of 80-poly(S-*r*-vinyldisiloxane). Degradation begins to occur at 200°C. This is indicative of the sulfur domains beginning to degrade.

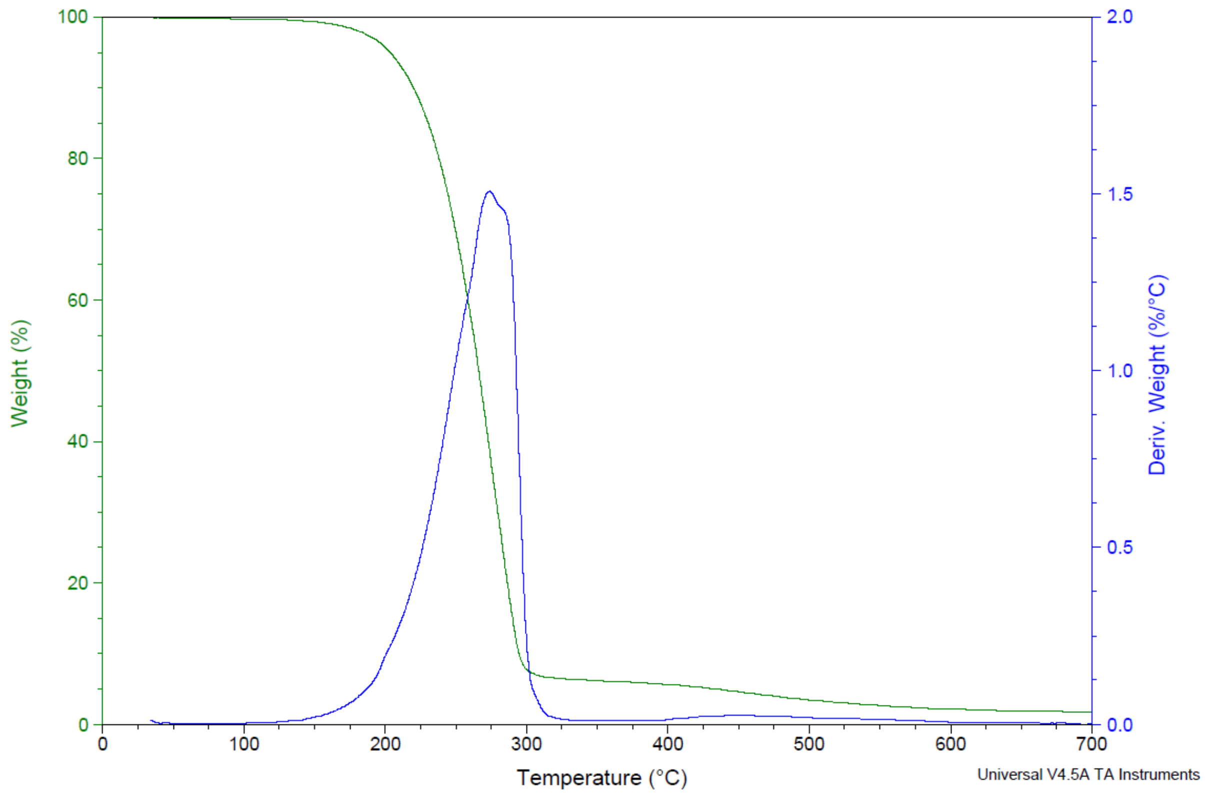

Figure S22: TGA scan of 90-poly(S-*r*-vinyldisiloxane). Degradation begins to occur at 200°C. This is indicative of the sulfur domains beginning to degrade.

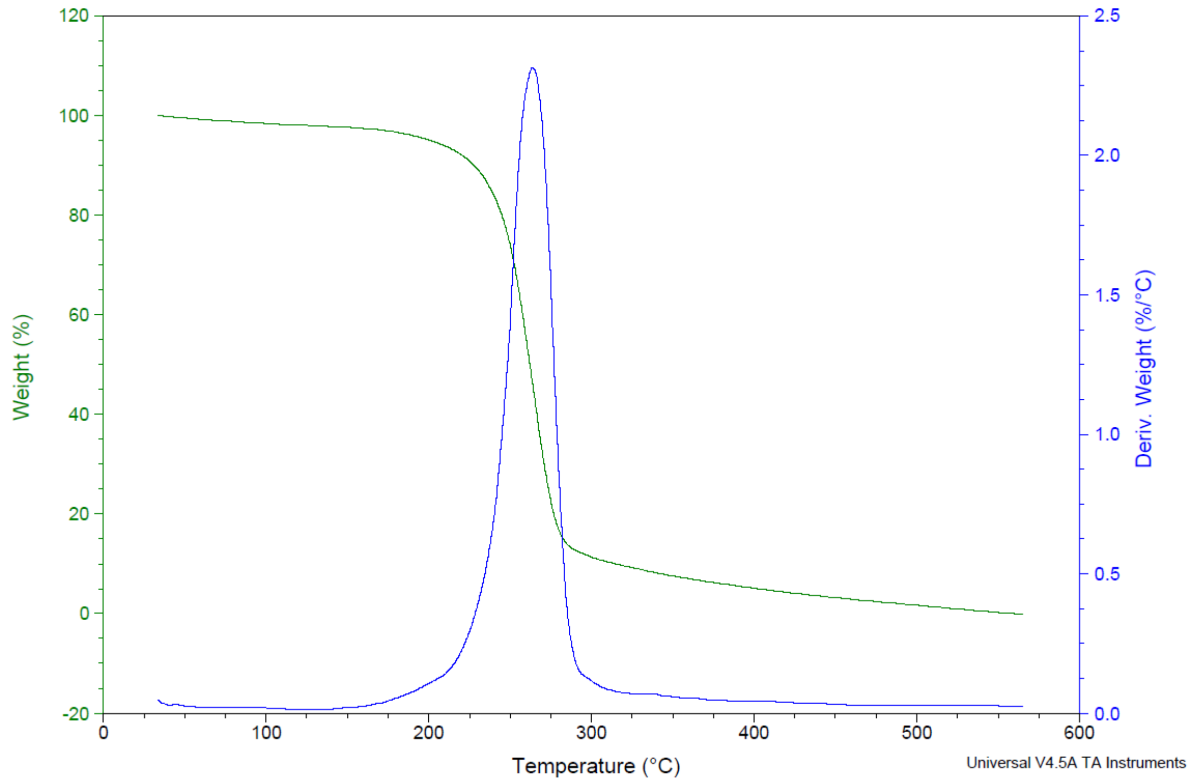

Figure S23: TGA scan of 40-poly(S-*r*-allyldisiloxane). Degradation begins to occur at 200°C. This is indicative of the sulfur domains beginning to degrade.

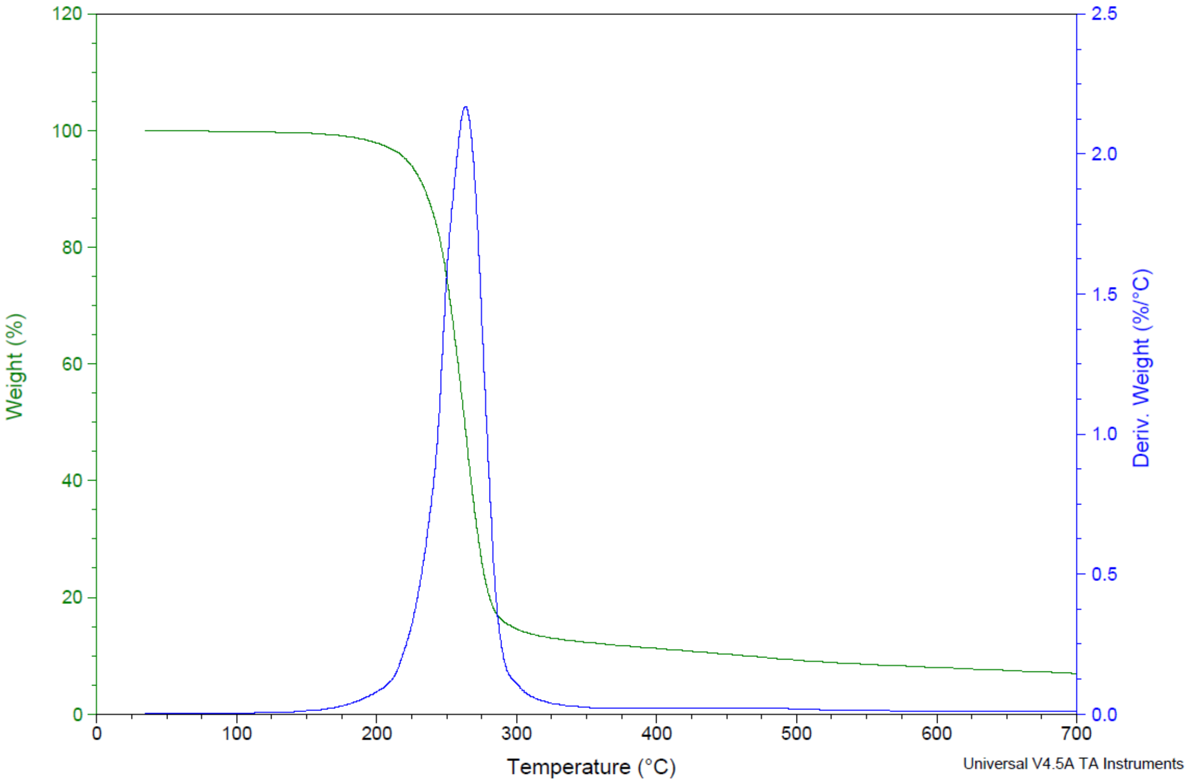

Figure S24: TGA scan of 50-poly(S-*r*-allyldisiloxane). Degradation begins to occur at 200°C. This is indicative of the sulfur domains beginning to degrade.

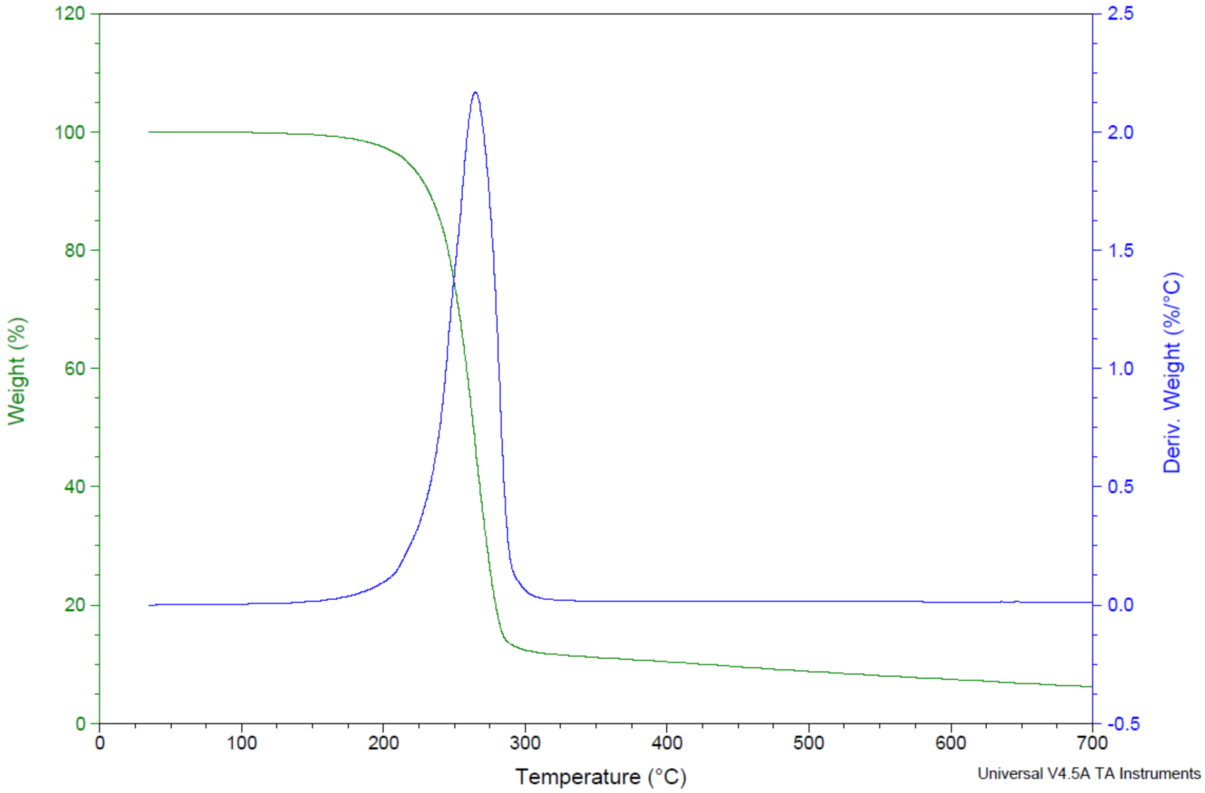

Figure S25: TGA scan of 70-poly(S-*r*-allyldisiloxane). Degradation begins to occur at 200°C. This is indicative of the sulfur domains beginning to degrade.

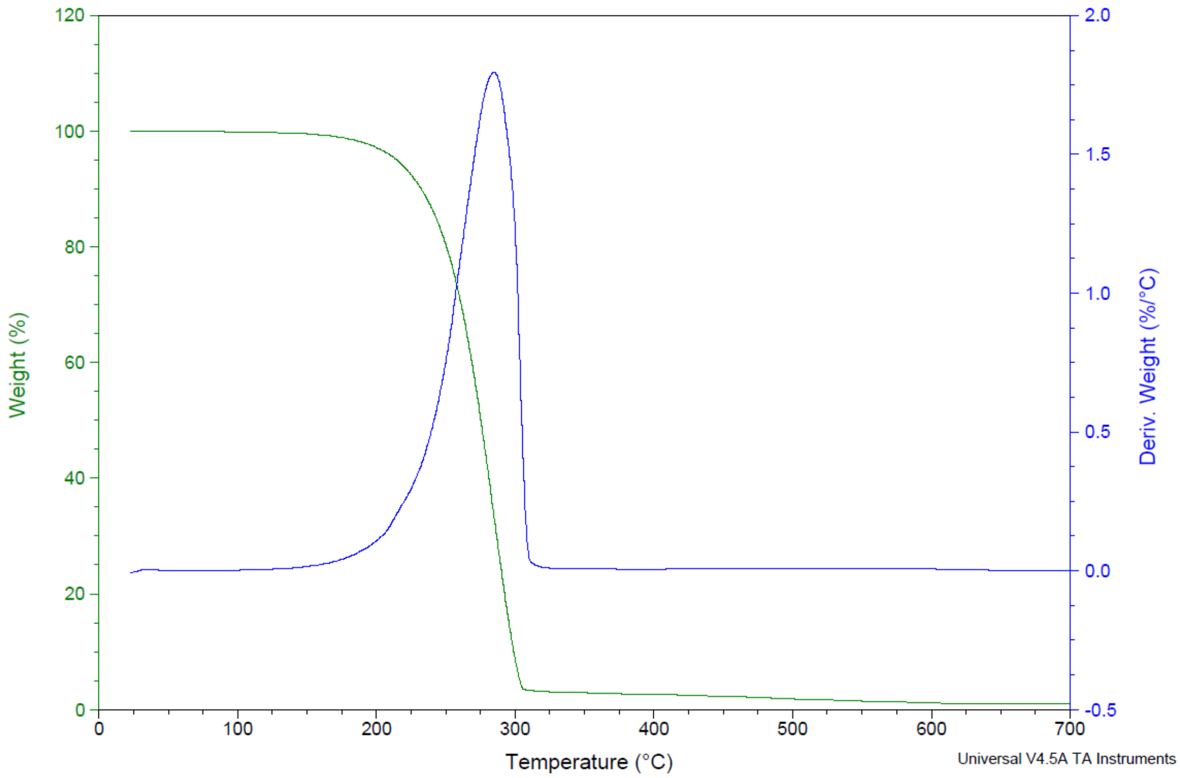

Figure S26: TGA scan of 90-poly(S-*r*-allyldisiloxane). Degradation begins to occur at 200°C. This is indicative of the sulfur domains beginning to degrade.

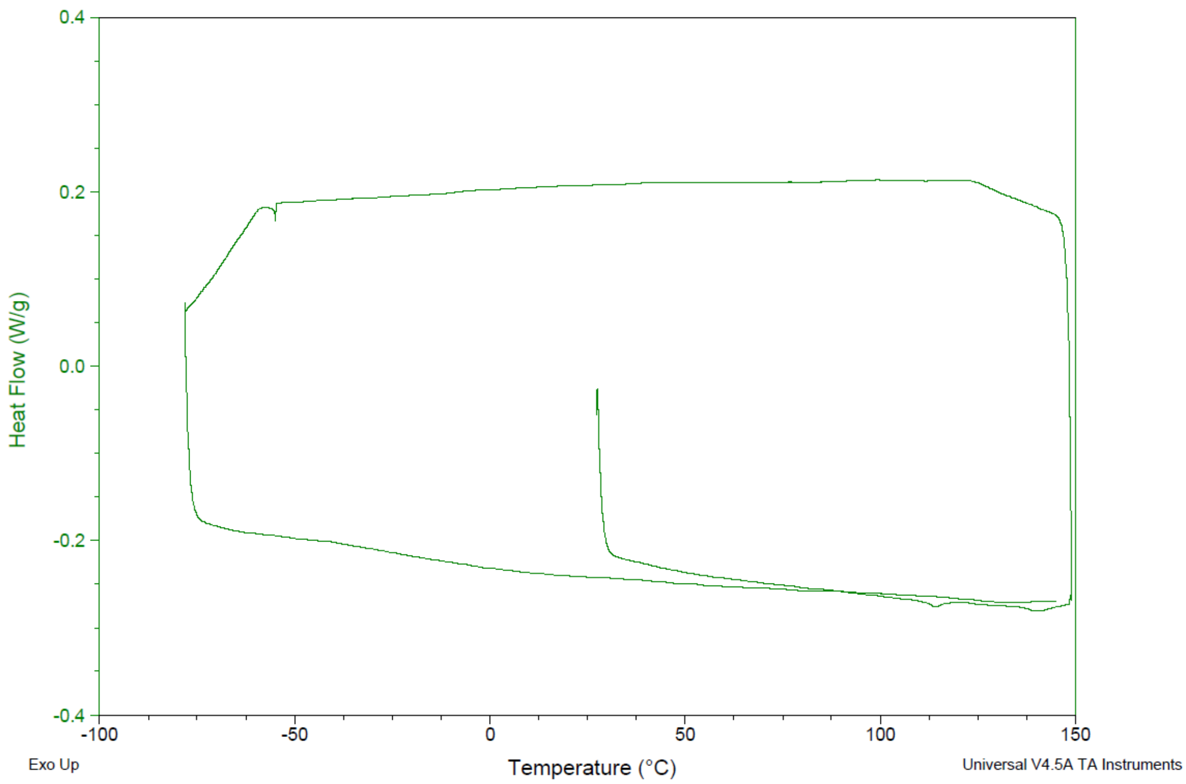

Figure S27: DSC scan of 30-poly(S-*r*-vinyldisiloxane). No T_g shown.

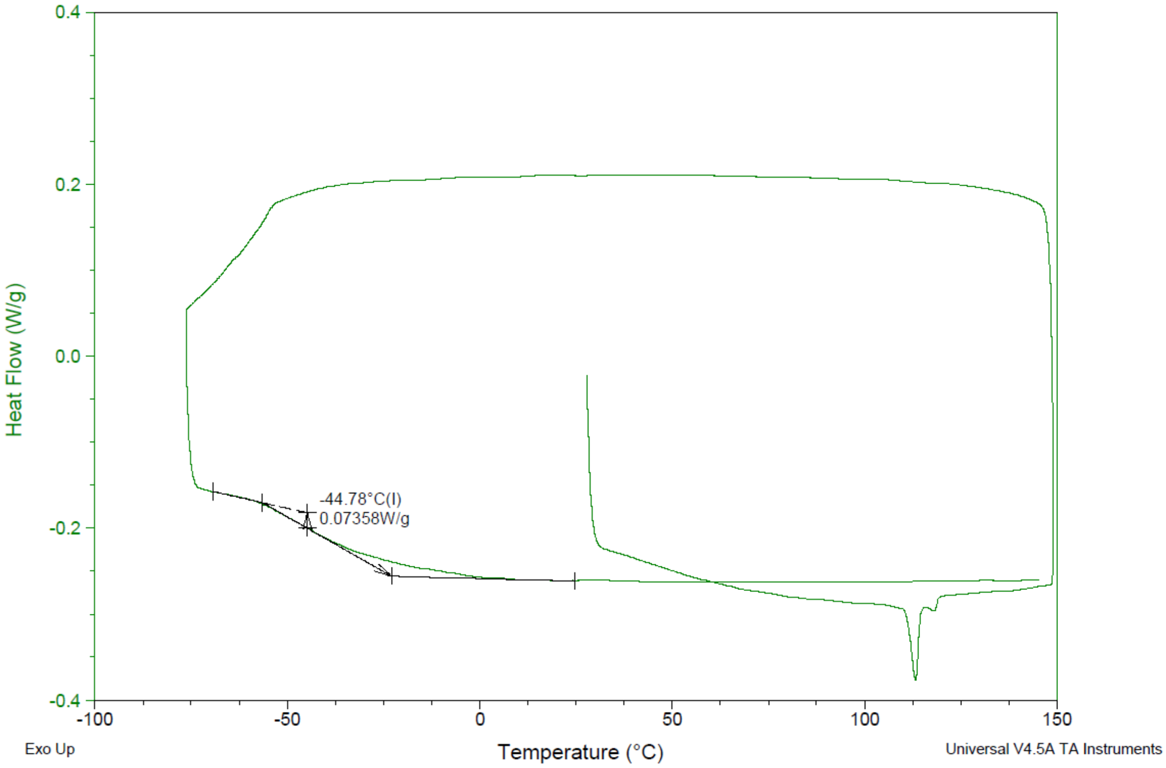

Figure S28: DSC scan of 40-poly(S-*r*-vinyldisiloxane). T_g shown at -44.8°C and unreacted elemental sulfur shown melting at 120°C.

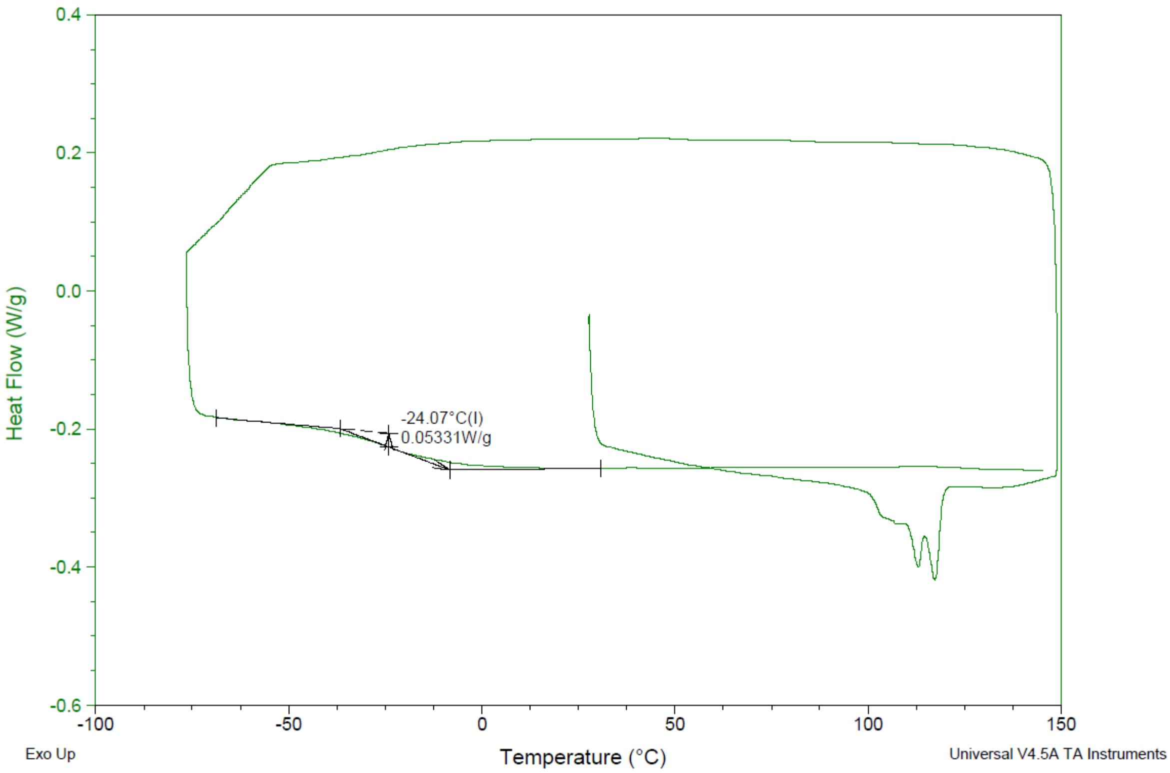

Figure S29: DSC scan of 50-poly(S-*r*-vinyldisiloxane). T_g shown at -24.1°C and unreacted elemental sulfur shown melting at 120°C.

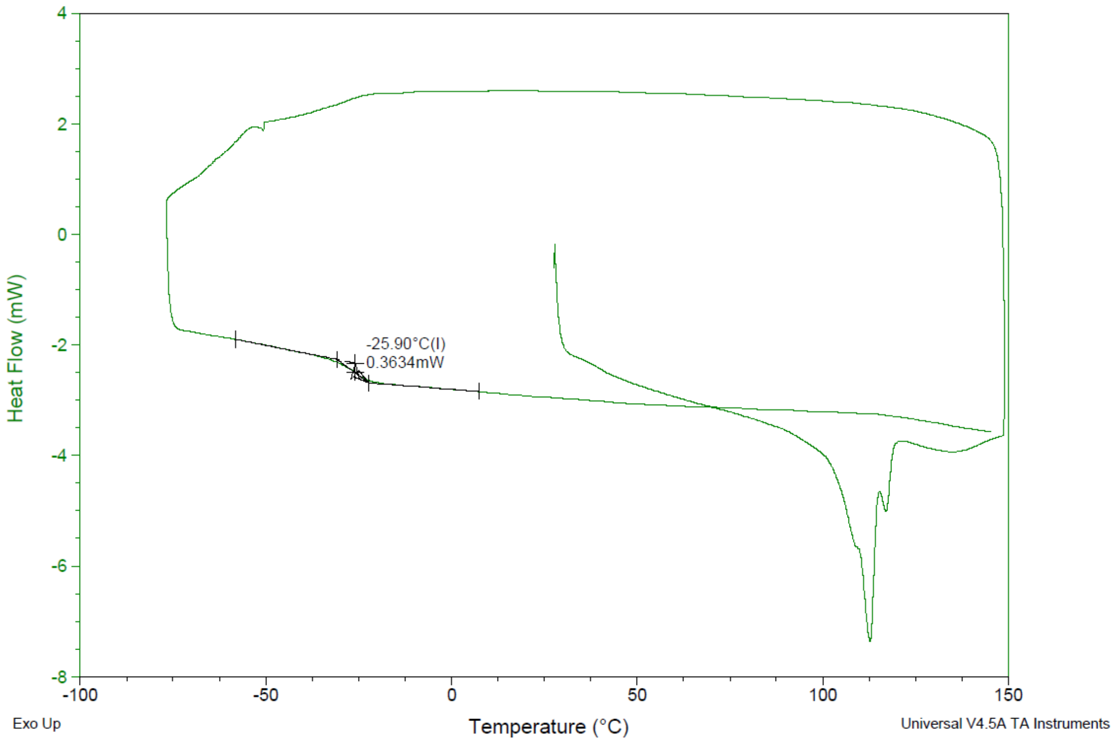

Figure S30: DSC scan of 60-poly(S-*r*-vinyldisiloxane). T_g shown at -25.9°C and unreacted elemental sulfur shown melting at 120°C.

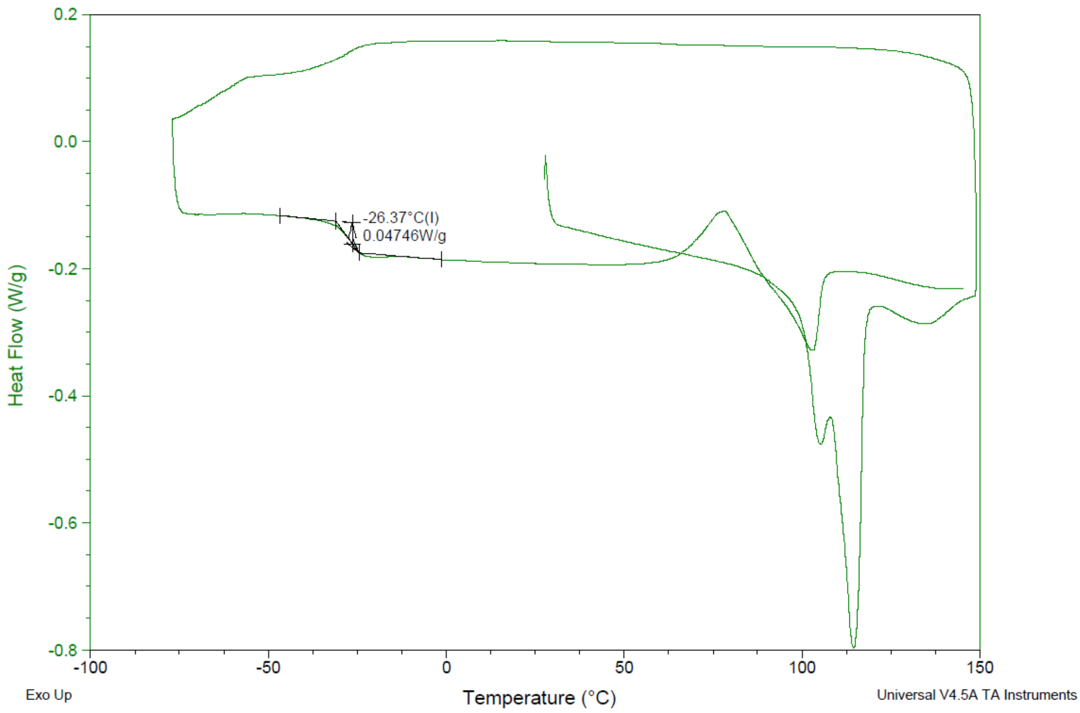

Figure S31: DSC scan of 70-poly(S-*r*-vinyldisiloxane). T_g shown at -26.7°C and unreacted elemental sulfur shown melting at 120°C.

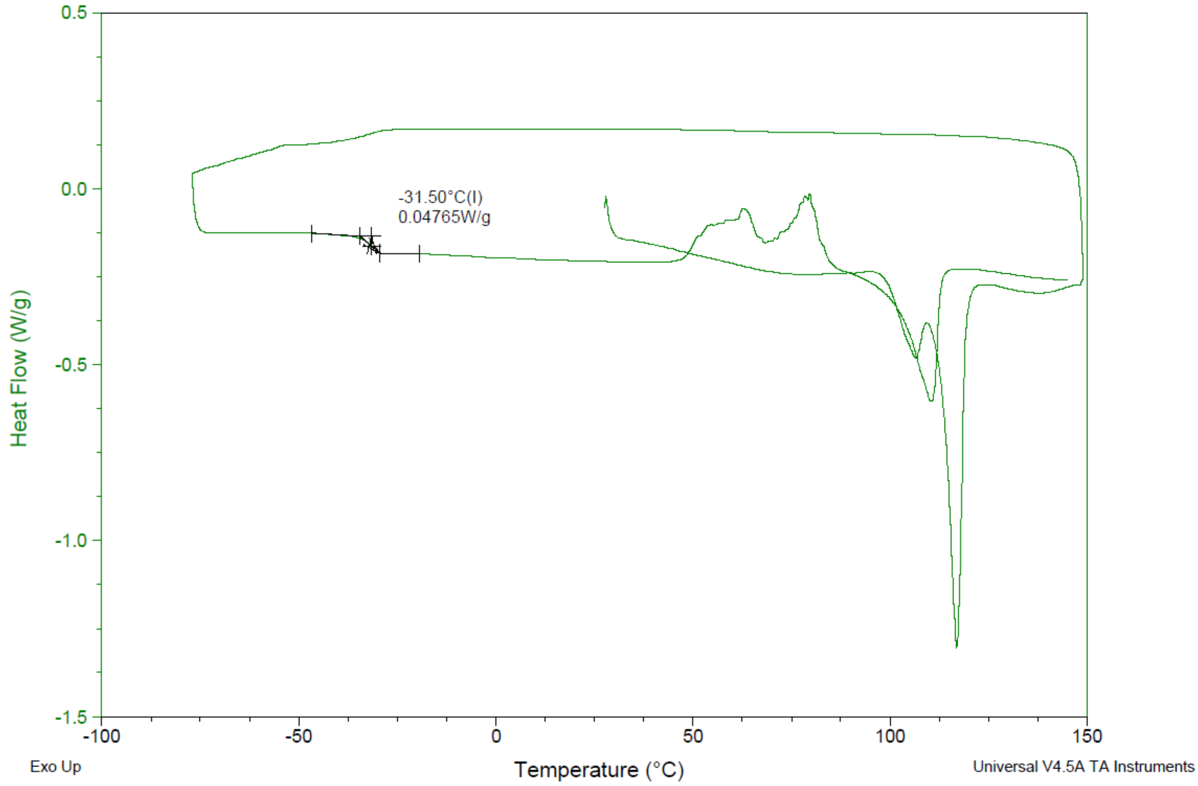

Figure S32: DSC scan of 80-poly(S-*r*-vinyldisiloxane). T_g shown at -31.5°C and unreacted elemental sulfur shown melting at 120°C.

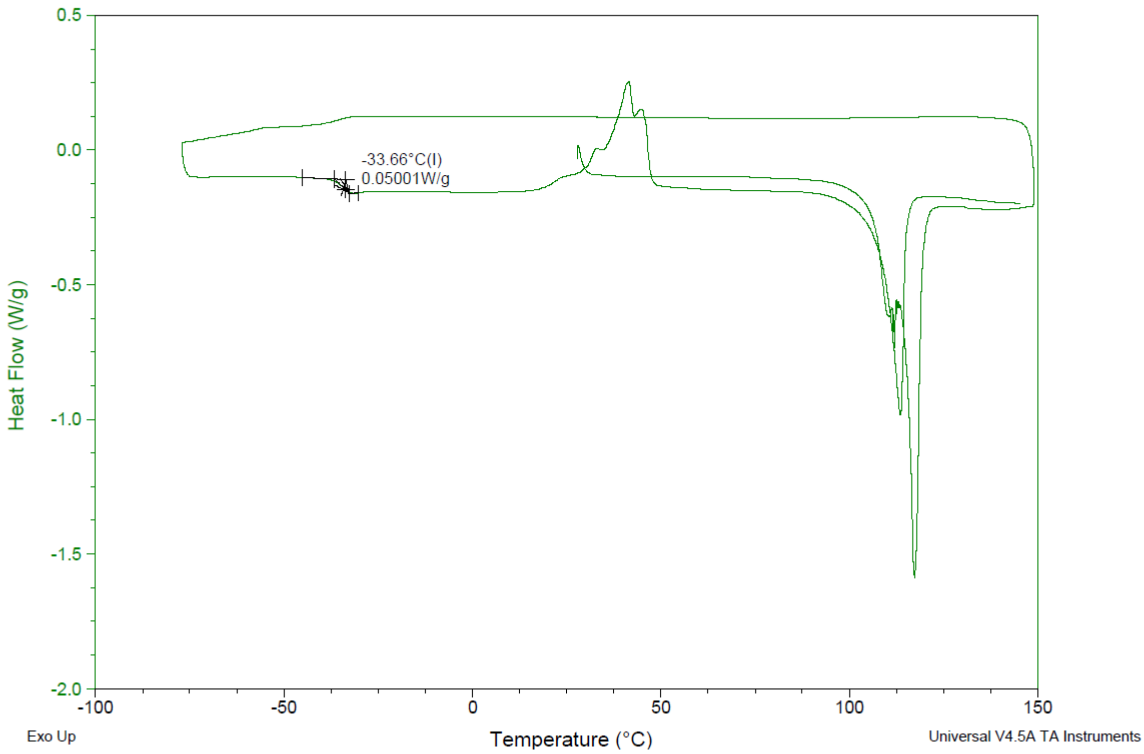

Figure S33: DSC scan of 90-poly(S-*r*-vinyldisiloxane). T_g shown at -33.6°C and unreacted elemental sulfur shown melting at 120°C.

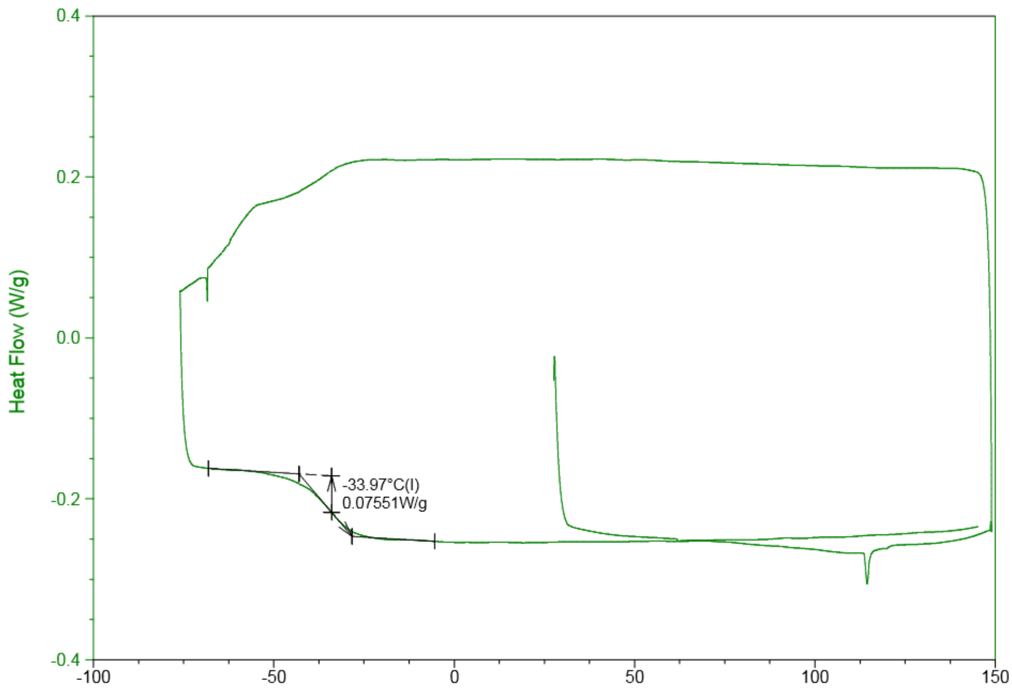

Figure S34: DSC scan of 40-poly(S-*r*-allyldisiloxane). T_g shown at -34.0°C and unreacted elemental sulfur shown melting at 120°C.

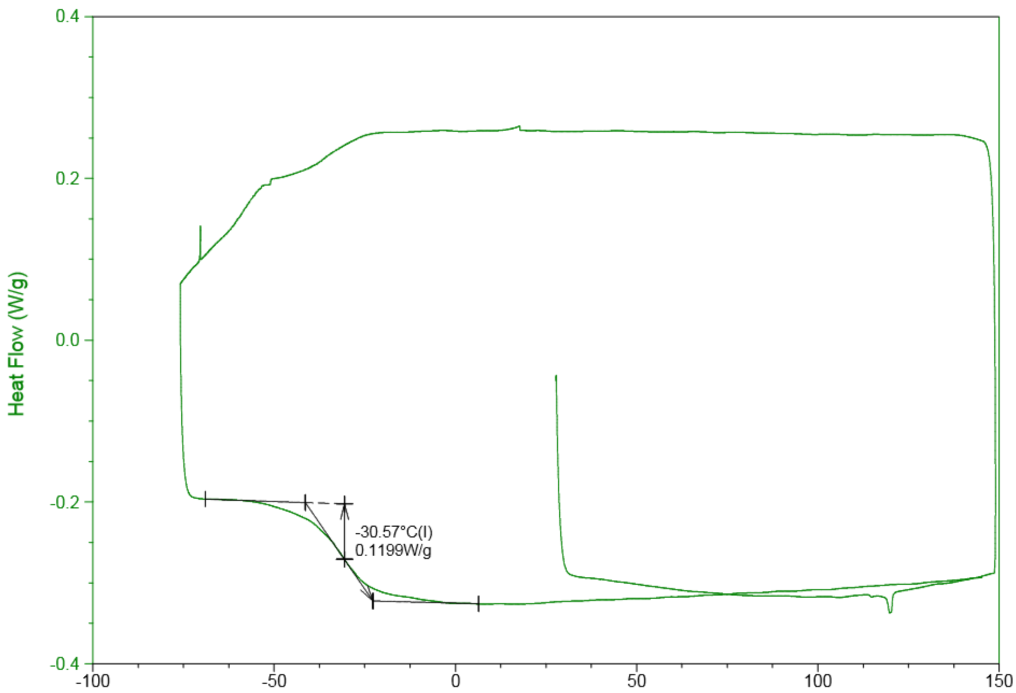

Figure S35: DSC scan of 50-poly(S-*r*-allyldisiloxane). T_g shown at -30.6°C and unreacted elemental sulfur shown melting at 120°C.

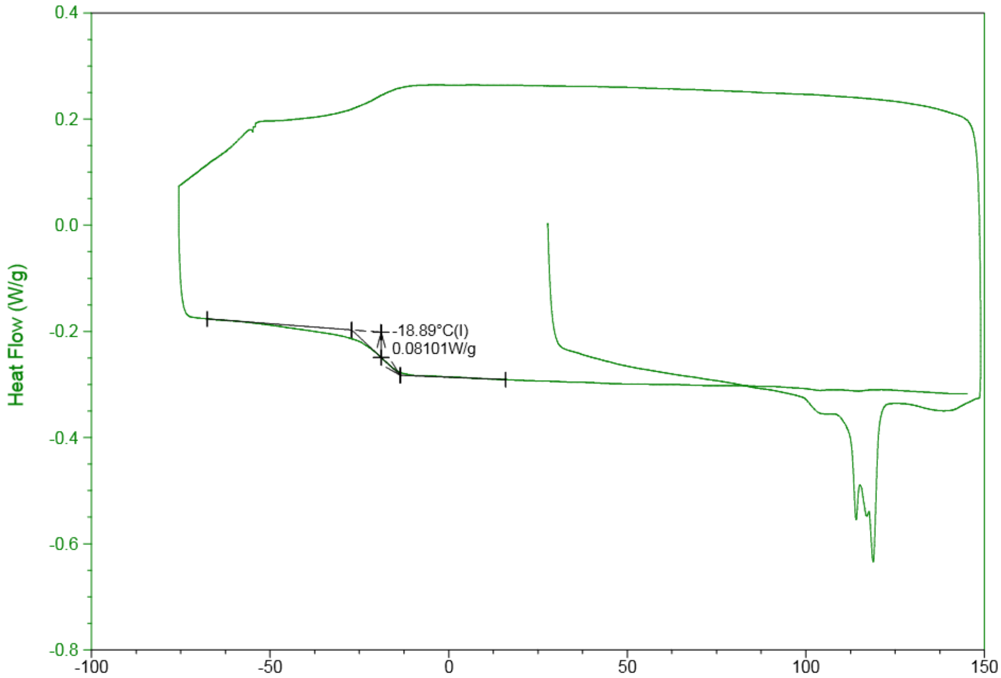

Figure S36: DSC scan of 70-poly(S-*r*-allyldisiloxane). T_g shown at -18.9°C and unreacted elemental sulfur shown melting at 120°C.

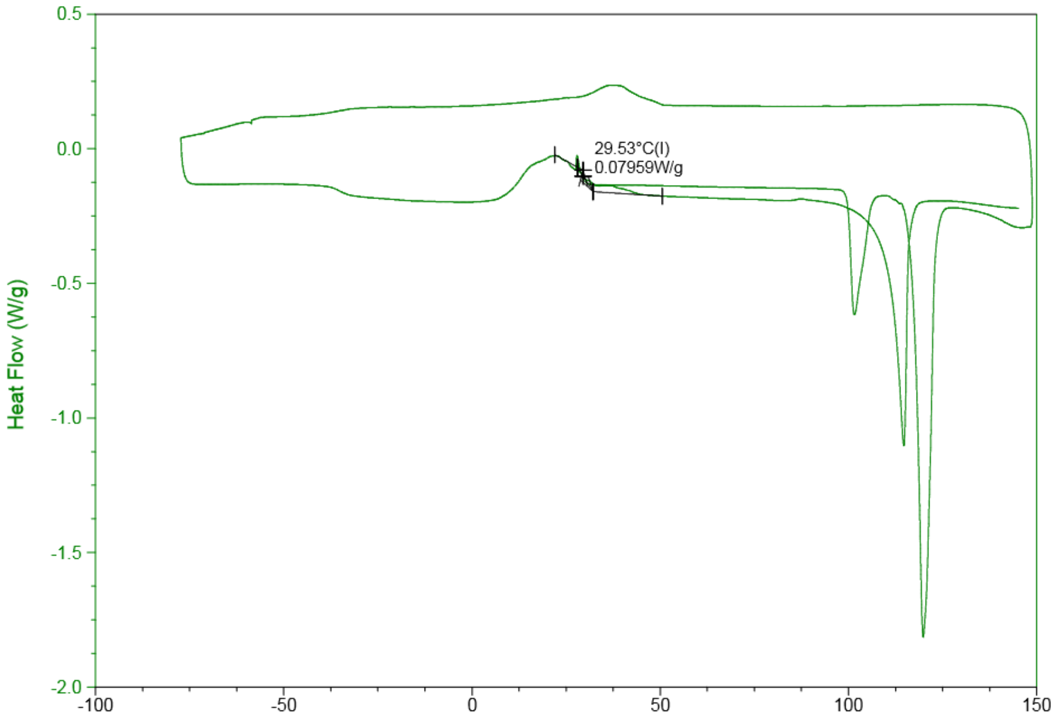

Figure S37: DSC scan of 90-poly(S-*r*-allyldisiloxane). T_g shown at 29.5°C and unreacted elemental sulfur shown melting at 120°C.

Table S1: Elemental analysis of the series X-poly(S-*r*-vinyldisiloxane), where X= wt% S.

Weight [mg]	X	Method	N [%]	C [%]	H [%]	S [%]
5.978	30	5 mg 90S	0.01	20.38	5.522	29.757
5.554	50	5 mg 90S	0.02	19.84	4.621	32.172
5.093	60	5 mg 90S	0.01	15.26	1.827	42.840
5.510	70	5 mg 90S	0.01	7.65	0.836	66.730
5.167	80	5 mg 90S	0.02	7.07	0.877	73.581
4.716	90	5 mg 90S	0.01	5.16	0.912	88.704

Table S2: Elemental analysis of the X-poly(S-*r*-allyldisiloxane), where X = wt% S.

Weight [mg]	X	Method	N [%]	C [%]	H [%]	S [%]
5.214	33	5 mg 90S	0	30.14	7.025	32.246
5.184	37	5 mg 90S	0	27.87	7.018	32.400
5.923	40	5 mg 90S	0	25.99	6.518	33.107
5.835	45	5 mg 90S	0	25.61	6.441	31.152
5.274	50	5 mg 90S	0	25.75	6.678	29.705
5.176	70	5 mg 90S	0	20.02	3.085	39.281

Table S3: Predicted elemental analysis of the series X-poly(S-*r*-vinyldisiloxane), where X= wt% S.

X	S rank	C [%]	H [%]	O [%]	S [%]	Si [%]
30	1.2461	36.14	6.82	6.02	29.9	21.2
40	1.939548	30.92	5.84	5.15	40.02	18.07
50	2.909516	25.76	4.86	4.29	50.03	15.06
60	4.364275	20.61	3.89	3.43	60.02	12.05
70	6.789002	15.45	2.92	2.57	70.02	9.03
80	11.63807	10.31	1.95	1.72	80.01	6.02
90	26.17161	5.15	0.97	0.86	90	3.01

Table S4: Predicted elemental analysis of the series X-poly(S-*r*-allyldisiloxane), where X= wt% S.

X	S rank	C [%]	H [%]	O [%]	S [%]	Si [%]
33	1.648206	37.5	6.92	5	33.04	17.54
37	1.964899	35.28	6.51	4.7	37.01	16.5
40	2.230109	33.6	6.2	4.48	40	15.71
45	2.737129	30.81	5.69	4.1	44.99	14.41
50	3.345554	28	5.17	3.73	50	13.1
70	7.806552	16.8	3.1	2.24	70	7.86
90	30.11076	5.6	1.03	0.75	90	2.62

Table S4: XPS Elemental analysis of 33-poly(S-*r*-allyldisiloxane)

element	Mw (g/mol)	atom %	mw x A%	atomic mass unit	wt%
C	12.0107	59.05	709.2318	1.17773E-21	42.15503453
Si	28.0855	16.81	472.1173	7.83987E-22	28.06151417
O	15.999	16.99	271.823	4.51383E-22	16.15650596
S	32.065	7.15	229.2648	3.80712E-22	13.62694534
total			1682.437	2.79382E-21	100

Table S5: XPS Elemental analysis of 40-poly(S-*r*-allyldisiloxane)

element	Mw (g/mol)	atom %	mw x A%	atomic mass unit	wt%
C	12.0107	59.42	713.6758	1.18511E-21	41.6546227
Si	28.0855	16.35	459.1979	7.62534E-22	26.80168848
O	15.999	14.72	235.5053	3.91075E-22	13.7455742
S	32.065	9.51	304.9382	5.06374E-22	17.79811462
total			1713.317	2.8451E-21	100

Table S6: XPS Elemental analysis of 45-poly(S-*r*-allyldisiloxane)

element	Mw (g/mol)	atom %	mw x A%	atomic mass unit	wt%
C	12.0107	59.74	717.5192	1.1915E-21	41.96382007
Si	28.0855	15.81	444.0318	7.37349E-22	25.96901686
O	15.999	14.67	234.7053	3.89746E-22	13.72664591
S	32.065	9.78	313.5957	5.2075E-22	18.34051716
total			1709.852	2.83934E-21	100

Table S7: XPS Elemental analysis of 50-poly(S-*r*-allyldisiloxane)

element	Mw (g/mol)	atom %	mw x A%	atomic mass unit	wt%
C	12.0107	59.54	715.1171	1.18751E-21	41.07854688
Si	28.0855	14.72	413.4186	6.86514E-22	23.74804661
O	15.999	13.28	212.4667	3.52818E-22	12.20474855
S	32.065	12.47	399.8506	6.63983E-22	22.96865796
total			1740.853	2.89082E-21	100

Figure S38: Microscopic image of polysulfide containing unreacted elemental sulfur on the surface.

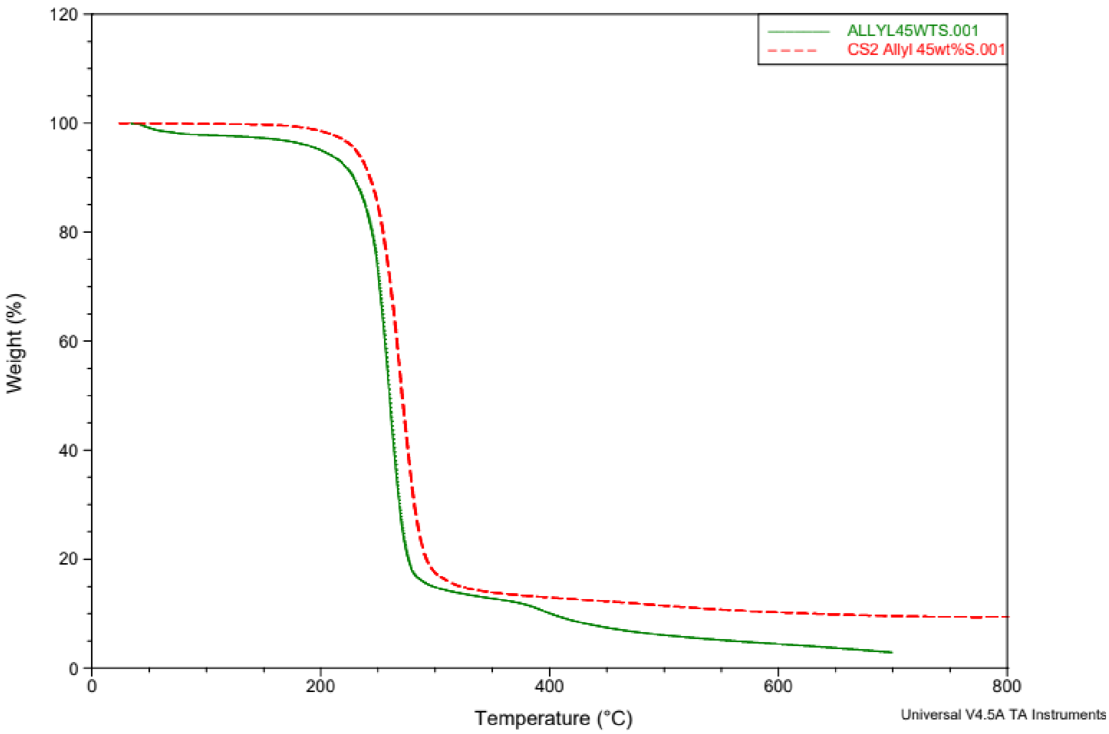

Figure S39: Comparison of TGA scans of CS_2 washed (red) and unwashed (green) 45-poly(S-*r*-allyldisiloxane).

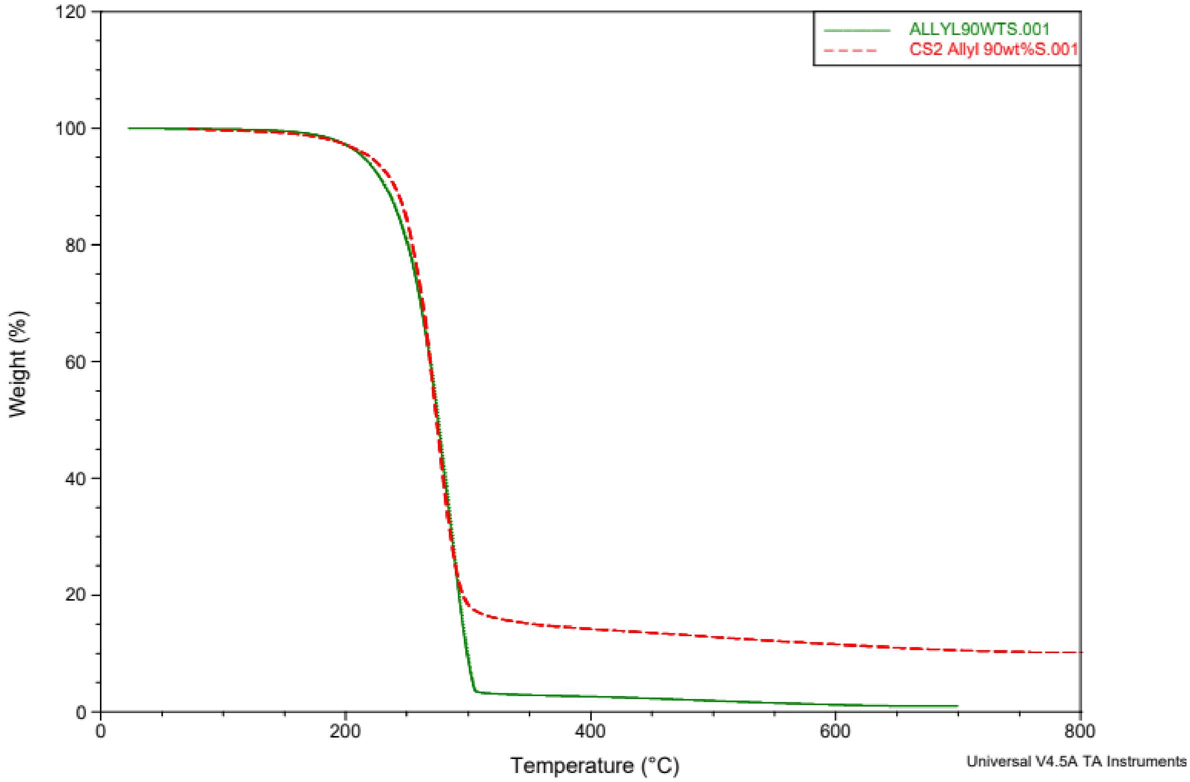

Figure S40: Comparison of TGA scans of CS_2 washed (red) and unwashed (green) 90-poly(S-*r*-allyldisiloxane).

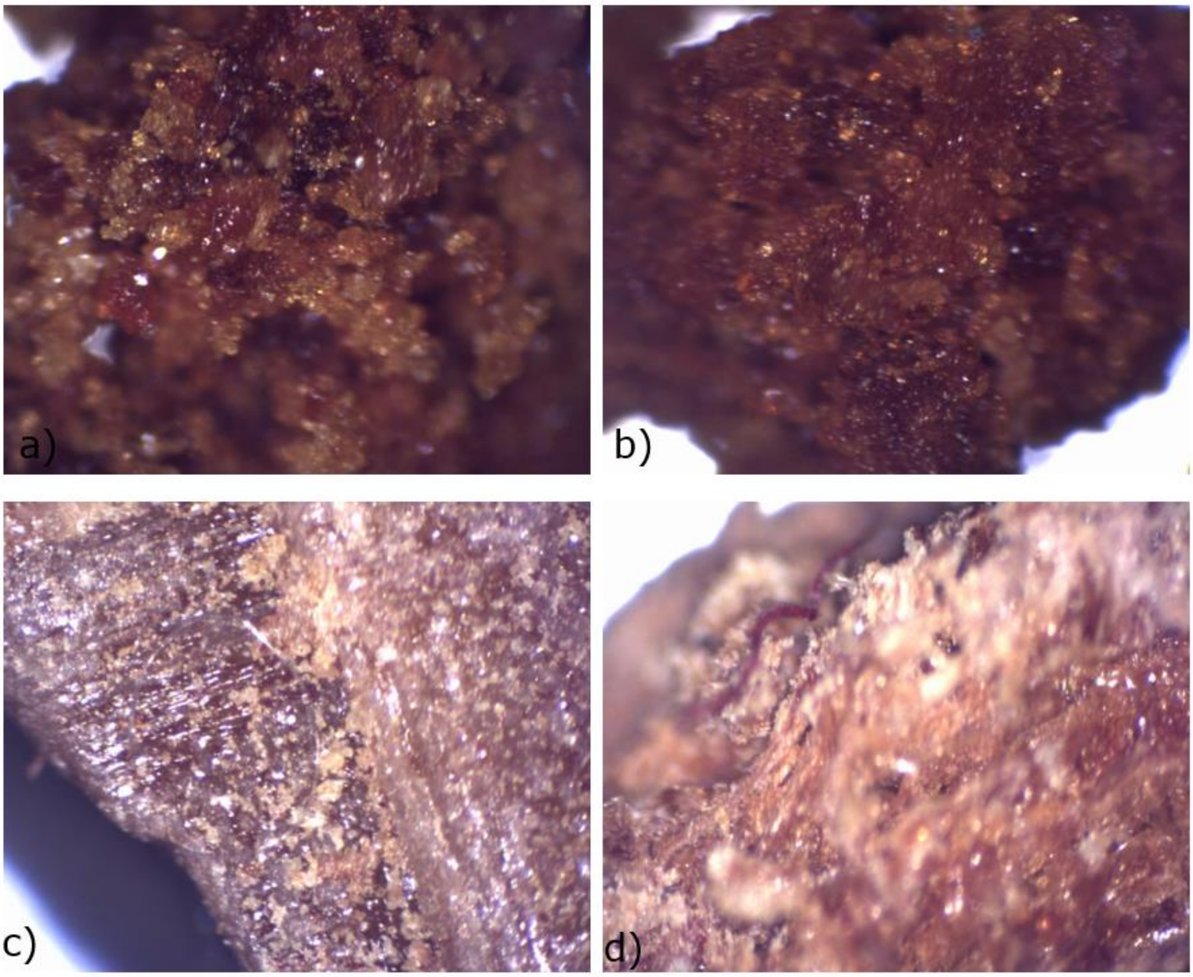

Figure S41: Optical microscopy of X-poly-(S-*r*-allyldisiloxane) series. a) X = 40 before and b) after CS_2 wash; c) X = 90 before and d) after CS_2 wash

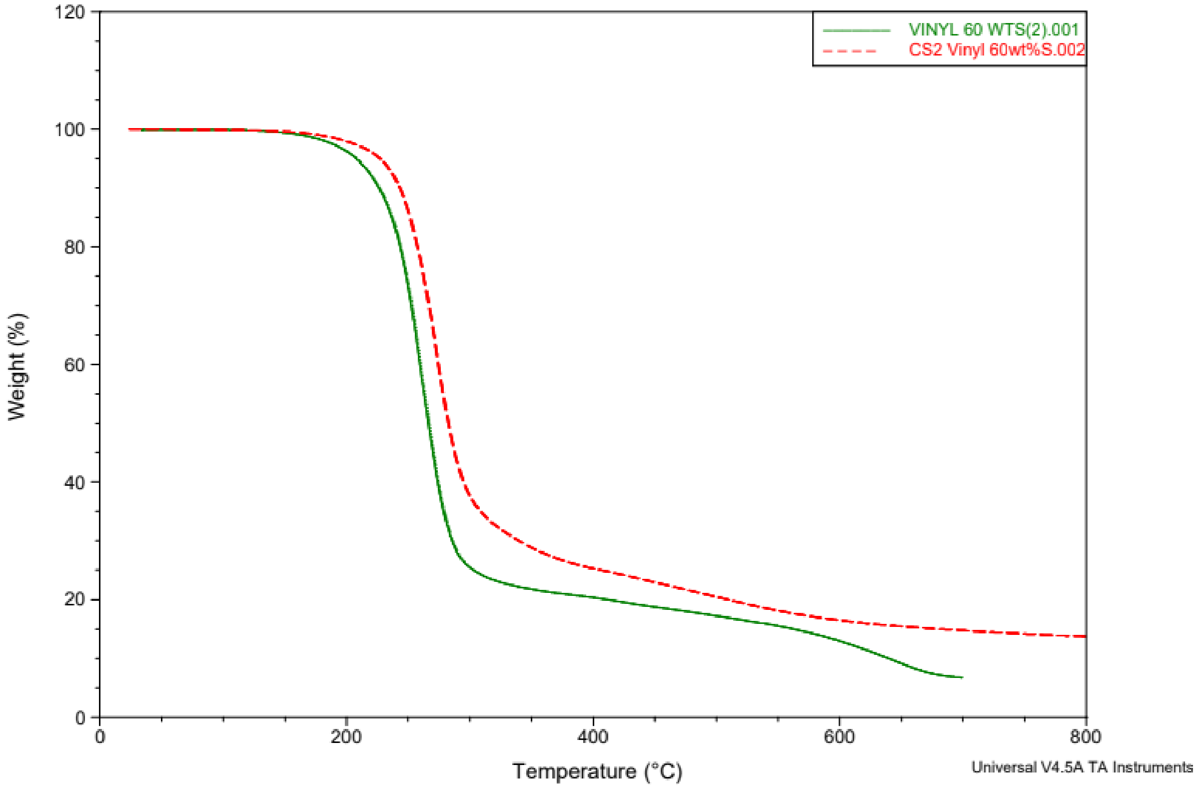

Figure S42: Comparison of TGA scans of CS_2 washed (red) and unwashed (green) 60-poly(S-*r*-vinyldisiloxane).